TAMPEREEN TEKNILLINEN YLIOPISTO
TAMPERE UNIVERSITY OF TECHNOLOGY

TARU SUONURMI

COMPONENT MOUNTING ON STRETCHABLE SUBSTRATE IN WEARABLE ELECTRONICS APPLICATIONS

Master of Science thesis

Examiners: prof. Jukka Vanhala,
Assoc. Prof. Matti Mäntysalo
Examiners and topic approved by the Faculty Council of the Faculty of Computing and Electrical Engineering on 9th March 2016

ABSTRACT

TARU SUONURMI: Component Mounting on Stretchable Substrate in Wearable Electronics Applications
Tampere University of Technology
Master of Science Thesis, 57 pages
March 2016
Master's Degree Programme in Electrical Engineering
Major: Electronics Product Design
Examiners: Professor Jukka Vanhala, Associate Professor Matti Mäntysalo

Keywords: wearable electronics, stretchable electronics, adhesives, strain testing, screen-printing

Wearable electronics is a new growing field of technology. Many companies have introduced wearable electronics applications, mostly related to the fields of fitness or healthcare. The wearable device should be able to be worn unobtrusively and safely. In order to guarantee those the stretchable electronics may be a more suitable option than conventional rigid electronics or even flexible electronics. One way to implement a stretchable electronics circuit is by miniaturizing functional modules to small rigid functional islands. The islands can be mounted on the stretchable substrate by an adhesive and connected to each other with stretchable interconnects.

In this thesis, the aim is to manufacture and evaluate adhesive joints of a different kind between the stretchable substrate and the rigid component. First in this thesis, the theoretical background of the stretchable materials, of the adhesives and of the manufacturing processes is studied. For testing the adhesive joints, the test samples with screen-printed interconnects are manufactured. Then the components are mounted on the substrates by adhesives and the initial electrical properties of the samples are measured. After that the uniaxial cyclic stretch test is implemented where the resistances of the samples are measured continuously using 4-point measurements. The one-time elasticity test is implemented only with the best combination of the adhesive and the substrate. In addition in this thesis, a custom-made test setup is designed and executed which aim is to stretch the sample for the same amount in every direction at the same time. The functionality of the setup is evaluated by comparing it with the other test setup.

There were two main quality issues related to the screen-printing process. Firstly, the ink cracked on one substrate and secondly, the impurities weakened the quality of the printed traces. Although the measured sheet resistance values of the ink were higher than in the datasheet of the ink was reported they were still sufficient for this thesis. Only the samples that had all the four measurement channels with an initial resistance lower than 110 Ω were accepted to the strain tests. In addition to the adhesive joint, the measurement included also the resistance of the component and of the small parts of the printed wires. During the strain test, the samples were stretched 10 % for 500 times. The variation between the samples was high, even with the samples with the same combination of the adhesive and the substrate. However, one adhesive performed better than the others. Thus, it was used also in the comparison between the test setups. With the custom-made test setup, the samples lost the connection with a lower uniaxial measured extension, so the setup functioned as expected.

TIIVISTELMÄ

TARU SUONURMI: Komponentin liittäminen venyvälle alustalle puettavan elektroniikan sovelluksissa
Tampereen teknillinen yliopisto
Diplomityö, 57 sivua
Maaliskuu 2016
Sähkötekniikan diplomi-insinöörin tutkinto-ohjelma
Pääaine: Elektroniikan tuotesuunnittelu
Tarkastajat: Professori Jukka Vanhala, Associate Professor Matti Mäntysalo

Avainsanat: puettava elektroniikka, venyvä elektroniikka, liimat, venytystestaus, silkkipaino

Puettava elektroniikka on uusi kasvava teknologian ala. Monet yritykset ovat esitelleet puettavan elektroniikan sovelluksia, enimmäkseen urheiluun ja terveydenhuoltoon liittyen. Puettavaa laitetta tulee pystyä pitämään päällä häiritsemättömästi ja turvallisesti. Jotta nämä voidaan taata, venyvä elektroniikka saattaa olla parempi vaihtoehto kuin tavallinen jäykkä elektroniikka tai edes taipuisa elektroniikka. Yksi tapa toteuttaa venyvä elektroniikkapiiri on miniatyrisoida toiminnalliset moduulit pieniksi jäykiksi toiminnallisiksi saarekkeiksi. Saarekkeet puolestaan voidaan liittää venyvälle alustalle liimalla ja yhdistää toisiinsa venyvillä johtimilla.

Tämän diplomityön tarkoituksena on valmistaa ja arvioida liimaliitoksia venyvän alustan ja jäykän komponentin välillä. Ensimmäisenä tässä työssä tutustutaan venyviin materiaaleihin, liimoihin ja valmistusmenetelmiin teoreettisella tasolla. Liimaliitosten testaamista varten valmistetaan näytteet, jotka sisältävät silkkipainotekniikalla valmistetut johtimet. Sitten komponentit liitetään alustoille käyttäen liimoja ja näytteiden alkuperäiset resistanssit mitataan. Tämän jälkeen näytteille tehdään yksiakselinen syklinen venytystesti, jossa näytteiden resistansseja mitataan jatkuvasti käyttäen nelipistemittausta. Maksimaalinen venymä – testi toteutetaan vain parhaalle liiman ja alustan kombinaatiolle. Lisäksi, työssä suunnitellaan ja toteutetaan erikoisvalmisteinen testijärjestelmä, jonka tarkoituksena oli venyttää näytettä samanaikaisesti joka suuntaan yhtä paljon. Sen toiminnallisuutta arvioidaan vertaamalla sitä toiseen testijärjestelmään.

Silkkipainoprosessiin liittyen ilmeni kaksi pääasiallista laatuongelmaa. Ensinnäkin käytetty muste halkeili yhdellä alustalla ja toiseksi epäpuhtaudet heikensivät painettujen johtimien laatua. Vaikka musteen mitatut pintaresistanssien arvot olivat korkeammat kuin musteen datalehdellä ilmoitetut, ne olivat silti kelvolliset tähän työhön. Testeihin kelpuutettiin vain näytteet, joiden kaikkien neljän mittauskanavan alkuperäinen resistanssi oli alle 110 Ω. Liimaliitoksen lisäksi mittaus sisälsi komponentin resistanssin sekä pienet osat painettujen johtimien resistansseista. Venytyskokeen aikana, näytteet venytettiin 500 kertaa 10 %. Näytteiden välinen variaatio oli huomattava, jopa saman liiman sekä saman alustan sisältävien näytteiden kesken. Kuitenkin yksi liima suoriutui selvästi paremmin kuin muut. Näin ollen sitä käytettiin myös testijärjestelmien vertailussa. Tuloksena vertailulle, näytteiden kontaktit hajosivat aiemmin kun käytettiin erikoisvalmisteista venytyslaitetta, eli järjestelmä toimi kuten oli odotettu.

PREFACE

This Master's thesis was done at Department of Electronics and Communications Engineering at Tampere University of Technology during 2015-2016. Work was carried out based on the research done in Research, competence and innovation center for elastic electronics –project which is funded by The Regional Council of Satakunta, The Town of Kankaanpää, Clothing Plus Oy and Tampere University of Technology.

I would like to thank my thesis examiners Professor Jukka Vanhala and Associate Professor Matti Mäntysalo for guidance and valuable feedback. I would also like to thank everyone in the TUT Personal Electronics group, M.Sc. Aki Halme, M.Sc. Pekka Iso-Ketola and M.Sc Emma Kaappa, for valuable guidance during this work. In addition, I would like to thank the entire Kankaanpää unit for the great working environment.

Lastly, I would like to thank my family and friends for the support during this work and my studies.

Kankaanpää, 24.5.2016

Taru Suonurmi

CONTENTS

LIST OF SYMBOLS AND ABBREVIATIONS

ACA	Anisotropic Conductive Adhesive
ACF	Anisotropic Conductive Film
ACP	Anisotropic Conductive Paste
CNT	Carbon Nanotube
ECA	Electrically Conductive Adhesive
ECG	Electrocardiography
FR-4	Flame retardant 4. A common dielectric material for printed circuit board
ICA	Isotropic Conductive Adhesive
IPA	Isopropyl Alcohol
NCA	Non-Conductive Adhesive
PCB	Printed Circuit Board
PDMS	Polydimethylsiloxane
PSA	Pressure Sensitive Adhesive
PU	Polyurethane
PVC	Polyvinyl Chloride
PVDF	Polyvinylidene Fluoride
TFT	Thin Film Transistor
TPU	Thermoplastic Polyurethane
UV	Ultraviolet

A	area
E	Young's Modulus
F	force
L	length
L_0	initial length
p	pressure
R	resistance
R_s	sheet resistance
t	thickness
W	width
ΔL	length change
ε	strain
ε_a	axial strain
ε_t	transverse strain
μ	Poisson's ratio
ρ	resistivity
σ	stress
∞	infinity

1. INTRODUCTION

Wearable electronics is a fast growing field of technology that provides new possibilities especially in the fields of medical healthcare and fitness. In 2015, the wearable electronics was $20 billion business and it is forecasted to grow up to almost $70 billion in 2025 [1]. The aim of wearable electronics is to add electronics to a part of individual's daily life by integrating it as a fixed part of a cloth or an accessory. Smart watches are an example of wearable applications that are gaining popularity. Comparing with mobile phones, smart watches can offer additional functionalities such as heart rate monitoring. On the other hand in the field of medical healthcare, for example wearable wireless electrocardiography (ECG) monitoring system is implemented and presented [2].

In many wearable electronics products, rigid or even flexible electronics are not suitable because the comfortable use of the product demands the material to adjust to the curves of a human body, which makes stretchable electronics a more suitable option. In addition to comfort, also unobtrusiveness and lightness are commonly important properties in wearable electronic devices. One of the key challenges in the stretchable electronics technology is to simultaneously achieve both excellent electrical performance and mechanical robustness. Depending on application, a stretchable integrated system has to be designed so that it maintains mechanical and electrical properties either under the high values of strain or only after the strain is released. One way to implement a stretchable electronics circuit is by miniaturizing functional modules to small rigid functional islands [3][4]. The islands can be mounted on the stretchable printed circuit board (PCB) by an adhesive and in order to connect the islands, stretchable interconnects are used between the islands [3][4].

This thesis is based on the research done in Research, competence and innovation center for elastic electronics –project, which is funded by The Regional Council of Satakunta, The Town of Kankaanpää, Clothing Plus Oy and Tampere University of Technology. One of the targets of the project is to move the research focus from assembling electronics on flexible substrates into stretchable substrates.

Focus of the research has been more in the stretchable substrates and manufacturing of stretchable interconnects [5][6]. So, this thesis continues the research by concentrating on the component mounting. The objective of this thesis is to manufacture and evaluate adhesive joints of a different kind between a stretchable substrate and a rigid component. Three types of adhesives are used: isotropic conductive adhesive (ICA), anisotropic conductive adhesive (ACA) and non-conductive adhesive (NCA). In addition to differences in conductivities, the adhesives differ in their curing methods. Three differ-

ent thermoplastic polyurethanes (TPU) are used as a substrate material. In order to evaluate the joints, the stretchable interconnects are manufactured by a screen-printing process by using a silver ink. Two strain tests are used to evaluate the electrical properties of the adhesive joints. Another aim of this thesis is to design a test setup that stretches a sample the same amount in every direction at the same time. The performance of that setup is evaluated by comparing it with another test setup.

In Chapter 2, the terms of wearable and stretchable electronics are illustrated. Also, the basic principles of the stretchable electronics are discussed. This includes reviewing the mechanics of elasticity, the manufacturing of the stretchable electronics system and the material selections of substrates, ink and adhesives. The manufacturing process consists of two main phases: screen printing and component mounting. In Chapter 3, the manufacturing process of test samples is illustrated and the experiment methods are presented, whereas Chapter 4 focuses on the results of the corresponding experiments and the comparison of two test setups. Finally, the conclusions of the methods and the results are presented in Chapter 5.

2. STRETCHABLE ELECTRONICS

The term wearable electronics refers to an electronic device that is integrated into a textile or an accessory so that it can be worn comfortably and safely on the body. Wearable devices include watches, glasses, contact lenses, e-textiles, headbands and jewelry for example. These devices may provide the same functionalities as mobile phones and laptop computers. Typically, they provide also additional functionalities such as sensory and scanning properties, which make them more sophisticated than hand-held technology. Well-designed wearable electronics is aimed to simplify individuals' daily lives. First wearable technologies were primarily used in the field of military technology. Nowadays, they are applied more to the fields of medical healthcare and fitness. [7] The wearable technologies are used for sensing physiological signals such as a pulse, a function of muscles and a level of a stress. In addition, one of the key properties is that the user can access the information in real time. In healthcare applications also a doctor may have the real time access to the data.

Wearable electronics should be worn so that it does not disturb the normal movement of the user and is not noticeable by others unless intended. Hence, conventional rigid circuit boards are replaced by stretchable circuits. Wearable electronics requires at least stretchable wirings on a stretchable substrate. Some parts of the circuit may still be rigid or flexible. The rigid parts may even be manufactured of FR-4 and they can be mounted on the stretchable printed circuit board for example by an adhesive. Nevertheless, in order to retain the elasticity of the device, rigid parts have to be miniaturized. In Figure 1 is presented a structure that has rigid functional component islands with stretchable interconnects. [3][4]

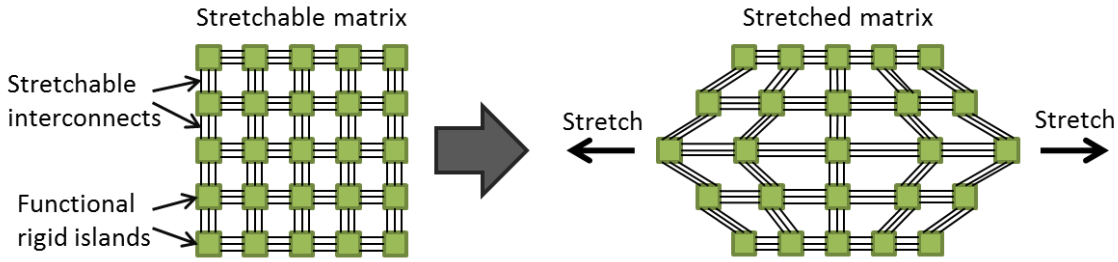

Figure 1. *Principle of stretchable circuit consisting of stretchable interconnects and functional rigid islands.*

A stretchable electronic device can be stretched without permanent impact on its initial shape. Additionally, stretching must not have much effect on the performance of the device. [8] Normally, a wearable device will experience most of the stress when the

cloth is dressed and undressed. Some applications require conductivity only when the cloth is worn on user's body and non-conductivity can be acceptable while the cloth is put on and taken off. However, the electronics should not make either dressing or undressing the cloth more difficult. The manufacturing of functioning and durable stretchable electronics requires more particularly from the electronics packaging methods and materials than the manufacturing of the conventional electronics. The electronics has to be cased so that it withstands physical stresses, washing and drying. On the other hand, the safety of electronics means that the device cannot heat up too much or cause electric shocks. In addition, the materials cannot affect the user negatively such as cause allergic reactions.

2.1 Mechanical Properties of Stretchable Materials

During material selection for an application, it is important to understand how stretchable materials behave in certain situations. When elastic material is stretched, a restoring force tends to bring it back to its original shape. However, as long as the material is not permanently deformed, it will always require the same force to stretch the material the same amount and it will return its original shape after the force is released. Linear elasticity can be expressed with Hooke's law:

$$\sigma = E\varepsilon\,, \tag{1}$$

where E is Young's Modulus, ε is strain and σ is stress. Young's Modulus is a constant that represents the stiffness of the elastic material. The bigger Young's Modulus is the stiffer is the material. The stress is mathematically defined by

$$\sigma = \frac{F}{A}, \tag{2}$$

where F represents the force that is applied to the material and A represents the cross-sectional area of the material. Whereas the strain is stated as

$$\varepsilon = \frac{\Delta L}{L_0}, \tag{3}$$

where L_0 represents the initial length of the material and ΔL is the change in length of the material caused by applied force. [9]

A stress-strain curve is another way to represent information about the material behavior. The curves of different materials may vary widely. However, an example of a stress-strain curve for an arbitrary material is illustrated in Figure 2.

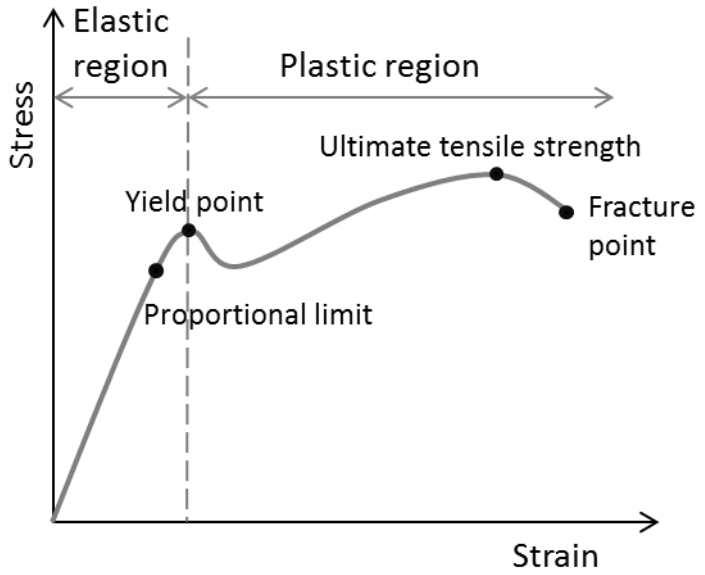

Figure 2. *An example of a stress-strain curve* [10]

The elastic region is the linear portion of the stress-strain curve. The slope of the line is defined by Young's Modulus. In this region, the material can be stretched and it will return to its original shape without any permanent transformation when the force is released. After the proportional limit the curve turns nonlinear and Young's Modulus cannot be used no longer. When the yield point is reached, material transfers from the elastic region to the plastic region. The plastic region is a region for permanent transformations. [9] After the yield point, the cross-sectional area of the material starts decreasing which also cause the stress to decrease. Then, if the strain is still increasing, also the stress increases again until it reaches the ultimate tensile strength. This is the maximum strength that the material can withstand. At this point, necking starts and the stress is decreasing until the material reaches its fracture point. [10]

On the other hand, when material is stretched, the material tends to change it geometry. In case of uniaxial stretching, the material elongates but also becomes narrower and thinner at the same time. Poisson's ratio describes this phenomenon and it can be described as

$$\mu = -\frac{\varepsilon_t}{\varepsilon_a}. \tag{4}$$

There ε_t represents transverse strain and ε_a represents axial strain. The transverse strain is negative for axial stretching and positive for axial compression, whereas the axial strain is positive for axial stretching and negative for axial compression. If the value of Poisson's ratio is 0, the material can be stretched uniaxial without affecting other dimensions. For most of the materials used in electronics Poisson's ratio is between 0.2 and 0.5. For many elastomers, the value is near to 0.5 and for metals the value is between 0.25 and 0.35. In stretchable electronics it is important to choose materials, which

Poisson's ratios are close to each other because mismatches at the interface with stress may cause failures by delamination. [11]

2.2 Stretchable Substrates

Comparing with conventional electronics, stretchable electronics requires new substrate material that is not just flexible but also elastic. Materials that enable stretching can be divided into three groups: plastic films, metal foils and fibrous materials. The fibrous materials include papers and textiles. Paper is used because of it is extremely cheap. However, both the papers and the textiles do not resist water or other solvents which may affect negatively on the electronics. The metal foils are a good alternative when high-temperature processing is required. The key disadvantages of the metal foils are weight and cost whereas plastic films are relatively inexpensive and light-weight. Metal foils are also less elastic than plastic substrates. Hence plastic films are the most used substrate material. [11]

However, new materials bring new challenges in the electronics fabrication process. Standard microfabrication processes cannot directly be used with stretchable plastic substrates. They have different operational temperatures and mechanical properties than typical rigid circuit boards. Additionally, in wearable electronics it is highly important that the substrate can be worn comfortably and safety. Elastomers are a typical choice for substrate in stretchable electronics due to their highly elastic properties. They can be deformed by applying mechanical stress and they still return to their original shape when the stress is removed. Polydimethylsiloxane (PDMS), polyurethanes (PU), polyvinylidene fluoride (PVDF) and acrylics are commonly used elastomers in stretchable electronics. [3]

PDMS that is also known as silicon rubber is widely used as a stretchable substrate. It is an ideal substrate because of its unique combination of properties. Silicon rubber has highly constant mechanical properties over a large temperature range. In addition, it is highly flexible material and both chemically and thermally stable. However, the surface tension of silicon rubber is low which may cause problems with printable electronics. [3]

Also polyurethane is highly elastic material. Typically, it can be stretched over 200 % before breaking. Moreover, some polyurethane materials can take even 1000 % elongation before breaking. On the other hand, high tensile strength with the elasticity is the reasons for the high abrasion resistance of polyurethanes. The abrasion resistance is even better with thermoplastic polyurethanes (TPU). In addition, TPU is known for its strength, toughness and elasticity. However, the temperature range of TPUs is quite low and the upper limit is typically between 80 and 120 ºC. At the upper temperature TPU becomes softer and it can be reformed and after cooling, it will remain in its new shape.

If even higher temperatures are needed, cast polyurethane is an alternative, but it cannot be reformed by heat like TPU. [12]

In this thesis, three different TPUs are used as a substrate material. One of them is Platilon® U 4201 by Epurex Films. It is an aromatic TPU based on polyether that is flexible over a wide temperature range and has a good adhesion to adhesives and inks. [13] Platilon is available in a relatively wide range of thickness. The selected thickness, 50 µm, comes from the lower end of the range. The reason of choosing this thickness is that the thinner material is more elastic than the thicker one. However, the thinness also makes the material more challenging to handle. Two other TPU substrates that are used in this thesis are called TPU1 and TPU2. Some properties of the substrates are presented in Table 1.

Table 1. *The properties of the substrates* [14] [15]

Property	**4201**	**TPU1**	**TPU2**
Density (g/cm^3)	1.15	NA	1.2
Softening range (ºC)	155-185	NA	155
Hardness (Shore A)	87	NA	95
Tensile stress at break (MPa)	60	NA	Warp: 67.0 Weft: 72.1
Tensile stress at 50% strain (MPa)	5-7	NA	NA
Tensile strain at break (%)	550	NA	Warp: 477 Weft: 507
Thickness (µm)	50	100	150

TPU1 consists of two layers. One layer is for the printing and the other one is the adhesive layer. The softening point of TPU1 is 105 ºC which means the temperature when the adhesive layer starts to flow. [16] Additionally, TPU1 is the only one of the substrates that has a carrier film.

2.3 Stretchable Interconnects

One of the major issues in creating stretchable electronics are interconnects. As they are placed on the stretchable substrate consequently they also have to be stretchable and remain their conductivity after stretching when they are returned to their initial shape. In some applications, they also have to retain their conductivity during stretching. The suitable materials for the conductors depend on the structure of wiring. In addition, different manufacturing processes require different properties of the wiring materials.

2.3.1 Structures of Wiring

The elasticity of the stretchable conductors can be enhanced by different patterning structures. They can be divided into in-plane and out-of-plane structures. Examples of out-of-plane structures are presented in Figure 3.

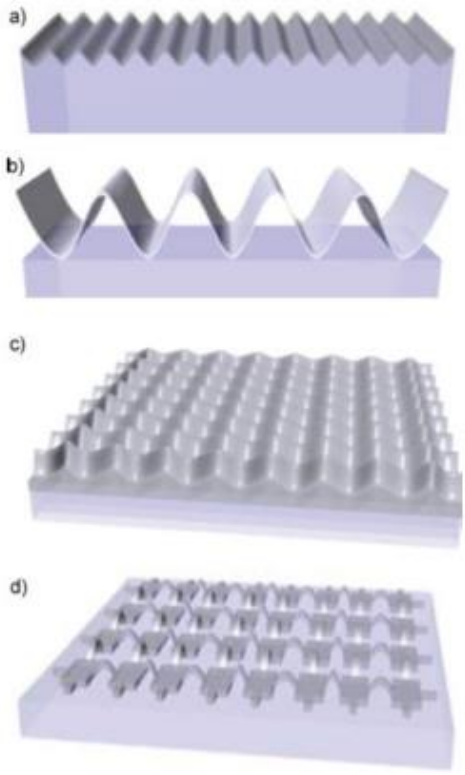

Figure 3. *Four out-of-plane structures: a) One-dimensional wavy ribbons b) A one-dimensional pop-up structure c) A two-dimensional wavy membrane d) A two-dimensional buckled mesh.*[17] *Reprinted with permission from John Wiley and Sons.*

For making out-of-plane structures, the stretchable substrate is first pre-stretched. In Figure 3a conductors are bonded at all points on their bottom on the substrate. When the stress is removed, the substrate can return to its original shape which causes bucking effect on the bonded conductors. That structure is known as stretchable wavy ribbons. Pop-up structure in Figure 3b is formed as previous but the conductors are bonded only at certain points. The advantage of this structure is that the range of elasticity can be optimized by specifying the wavelength of the structure. On the other hand, pop-up structure does not offer mechanical support for the whole conductor, only for the bonded points. [17]

However, the structures of Figure 3a and 3b present only the basic mechanics aspects. They are not actually suitable for electronics technology because of difficulties in forming connects or other elements directly on the substrate. In Figure 3c, there is a two-

dimensional wavy membrane and in Figure 3d a two-dimensional buckled mesh. There rigid device islands are bonded to the substrate and stretchable interconnects are bonded only loosely on the pre-stretched substrate. When pre-stretch is released, interconnects are buckled out of the surface. [17][18]

In-plane structures can be formed with a single line or with a meander structure. The single line structure is used in conventional electronics but in stretchable electronics it requires an intrinsically elastic conductive material. However, metals are still a worthy option for electronics interconnects due to their high conductivity and a relatively low cost. They are also established material in electronics technology though their elastic features are much weaker than polymers have. Therefor different meander shapes are also used as interconnects. [4] In Figure 4 typical types of meanders are illustrated: a triangular shape, a square shape, a "U" shape and a horseshoe shape.

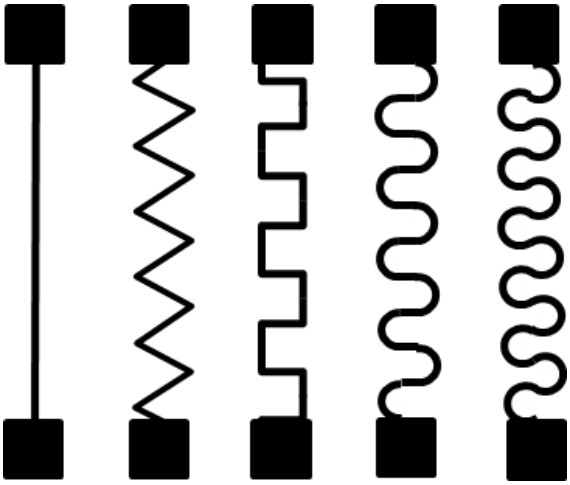

Figure 4. *In-plane structures: a single line, a triangular shape, a square shape, a "U" shape and a horseshoe shape*

All meander shapes provide better deformation than the straight line. However, in the conductors with triangular and the square shapes the stresses are relatively high at the sharp corners of the structures. The corners are eliminated in the "U"-shaped design but stresses are still concentrated in the small areas of the curves. Thus the horseshoe-shaped design is the most optimal of the meander shapes because the stress area is distributed in wider parts of the conductor. [4]

2.3.2 Manufacturing of Stretchable Interconnects

Photolithography has been a leading patterning technology in rigid electronics industry for nearly 50 years. However, the photolithography has come across new challenges with the new patterning materials of the stretchable electronics. Instead printing technologies provide cost-effective processing at a lower temperature that is also compatible with stretchable plastic substrates. In addition, printing is an additive technology, which make it more environmental friendly. There are several printing technologies available.

One of them is screen-printing that is widely used in printed electronics and it is used also in this thesis. [19]

The screen-printing provides several advantages over the other printing methods. The equipment is relatively cheap and readily available. There is also possibility of printing relatively thick layers which enable printing the highly conductive structures with conducting polymers. In addition, the screen printing requires only a little ink, so the waste of the ink is minimized. One disadvantage of the screen-printing is that it is not suitable for high-volume processing in the raw. However, the volume can be increased significantly by using rotary screen-printing. [19] [20]

A screen-printer consists of four main elements. They are a screen that defines the patterns, printing paste that forms the patterns, a surface where the patterns are created and a squeegee that forces the paste through the screen to the surface. The principle of the screen-printing process is shown in Figure 5. In the process, firstly, the substrate is placed on the nest and paste is applied in the front of the squeegee. Then the squeegee is pressed down so that the screen yields slightly down and touches the substrate. The squeegee moves on the screen and pushes the paste through the holes of the screen to the substrate. On the other end of the screen, the squeegee stops and is arisen. Eventually, the defined patterns are formed on the substrate. [21]

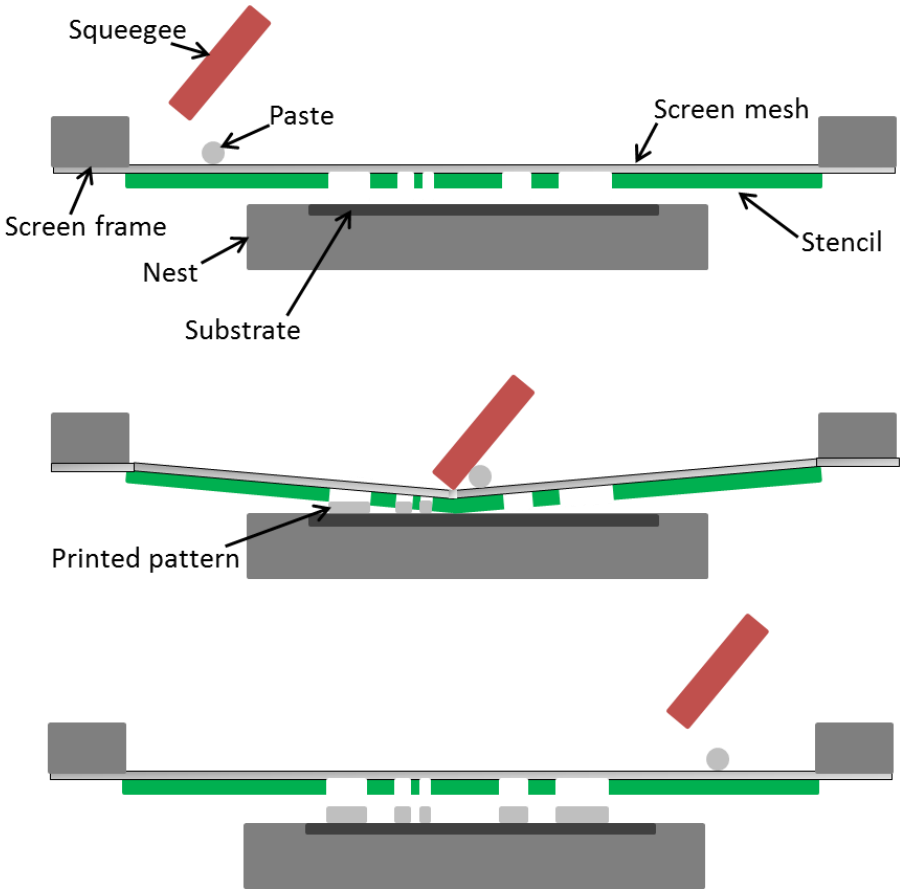

Figure 5. *The principle of the screen-printing process*

The screen consists of three parts: a frame, a mesh and a stencil. The role of the frame is to support the mesh. The frame is usually made of metal such as aluminum due to its strength and stability. The mesh is there to support the stencil. Polyester is the most used mesh material in industrial screen-printing but also nylon and stainless steel are used. Several properties characterize the mesh: the number of threads per centimeter, mesh opening, open area, thread diameter and cloth thickness. When choosing a mesh, there are two rules of thumb to use. Firstly, the minimum printed line width is three times the mesh thread diameter. Secondly, the mesh opening has to be at least three times the particle size of the ink paste. Additionally, cloth thickness is approximately two times the thread diameter. The last part of the screen, the stencil, defines the printed pattern. The stencil also directly affects the print thickness. A thicker stencil also means a thicker print layer. [21]

The squeegee presses the screen down into contact with the substrate, pushes ink through the stencil on the substrate and cuts the extra ink. Rubber, neoprene and polyurethane are the most common materials for the squeegee. In addition, various squeegee shapes are possible: square edged, single diamond and double diamond. The angle of the squeegee can vary but commonly it is around 45º. The squeegee has to be at least 10 mm wider than the print pattern on both sides because the screen tension tends to raise the ends of the squeegee. On the other hand, overly wide squeegee reduces the life of the screen because it overstretches the screen. [21]

2.3.3 Functional Electronic Inks for Stretchable Interconnects

In order to use the straight lines as interconnects, the material of interconnects has to be extremely elastic and to have extremely high electrical conductivity. Various printing methods also require different properties of the conducting material. In addition to the viscosity and the surface tension of the material, also compatibility with surrounding materials and tools has to be taken into account. Some metals have already established themselves in printing technologies. The most studied and used metal is silver because of its good electrical and physical properties on plastic substrates. However, silver is a precious metal and is not suitable for low cost electronic devices. Carbon and copper based inks are alternatives for silver. The biggest problem with copper is oxidation. In addition, two types of conducting polymers are used: intrinsically conductive polymers and polymers based on nanocomposites. Nanocomposite materials are made by mixing metallic nanoparticles with organic elastomers. The most studied nanocomposites are graphene and carbon nanotubes (CNT). [20]

In the screen-print technology it is important that the ink is compatible with the screen and the squeegee materials. On the other hand, screen-printing requires high-viscosity ink because lower viscosity inks would simply run through the mesh and the print pattern would be inaccurate. [20] A screen-print suitable ink, CI-1036 by ECM, is used in

this thesis. It is extremely flexible and highly conductive silver ink. In addition, it can be cured at 120 ºC that is lower than the softening range of the substrate materials. [22]

2.4 Rigid Component on Stretchable Substrate

Soldering has been the most used method for attaching a component to a substrate in electronics industry. However, solders cannot be used in the field of printed electronics. There are material incompatibilities between silver inks and solders because of the leaching effect of the solder material. The leaching behavior exists also with conventional printed copper structures but the phenomenon is much lighter than with the silver ink. Adhesives do not have the same effect so they are more compatible with silver inks. [23]

On the other hand, stretchable plastic substrates cannot handle as high temperatures as conventional PCBs. Typically electrical conductive adhesives (ECA) have lower processing temperatures than solders but there are also low-temperature solders available. However, indium, that can be used as a primary constituent in low-temperature solder, is very expensive which also makes the indium solders extremely expensive [24]. Therefore, the ECAs are also more suitable for low cost fabrication. However, the adhesives lack the self-alignment properties which could fix minor misalignment errors. The ECA joints are also harder to rework than the solder joints.

There are two types of ECAs: isotropic conductive adhesive (ICA) and anisotropic conductive adhesive (ACA). Both ECAs consists of a polymer binder and conductive particles. The concentration of the conductive particles defines if the adhesive is isotropic or anisotropic. ICA has the high concentration of the conductive particles thus it is electrical conductive in every direction. As for ACA, it has the low concentration of the particles and conducts only in one direction after the bonding process. Also, non-conductive adhesive (NCA) can be used to create both a mechanical and an electrical connection. In NCA connection the pads of the component are pressed against the pads in the substrate and the NCA only surrounds the joints.

2.4.1 Isotropic Conductive Adhesive with Underfill

Isotropic conductive adhesive is formed by adding enough conductive filler into a polymer matrix. Thus the polymer insulator transforms into a conductive material. A percolation theory has been used to explain the transformation. When the concentration of the conductive filler in the polymer matrix is increased, the resistivity of the material drops dramatically. The concentration of the conductive filler at that point is also called as a percolation threshold. After the percolation threshold, the further increase in the concentration decreases only a slightly the resistivity. However, the concentration cannot be increased too much because the polymer matrix provides the mechanical support

for the connection. [25] In Figure 6 is illustrated a typical cross section of an ICA connection.

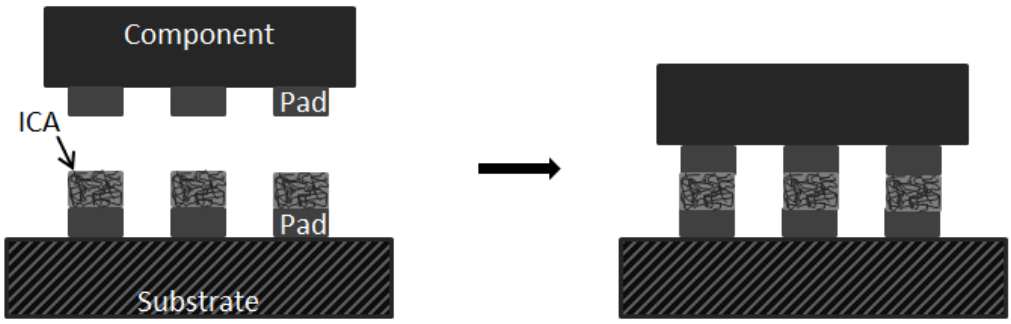

Figure 6. *A schematic illustration of ICA joints*

Silver-filled epoxies are commonly used in electronics industry as an ICA material because they offer good adhesive strength and thermal stability. In addition, they can retain these properties under demanding conditions. Silver is the most commonly used filler material because of its excellent conductivity, chemical stability and its oxide is highly conductive. [26]

Two-component silver epoxy adhesive, DB-1561 by ECM, is used in this thesis. It has excellent adhesion and it is compatible with the conductive ink used in this thesis. In addition, DB-1561 has a short and low temperature cure time. [27]

In order to improve the reliability of the joints, underfill can be used around the contact pads. Underfill UF-9526 by ECM is compatible with the ICA and the ink that are used thus that underfill was chosen. It also provides excellent adhesion fast with low temperature curing. [28] Typical forced curing time is 10 minutes at 110 ºC and respectively the same curing time and temperature can be used with DB-1561 [27][28]. Higher temperatures can typically reduce the curing time and improve the adhesion.

2.4.2 Anisotropic Conductive Adhesive

In an anisotropic conductive adhesive, the concentration of the conductive filler is below the percolation threshold. Thus the adhesive does not conduct before the interconnections are formed. The amount of conductive particles is typically between 0.5 % and 5 % of the total volume of ACA. The amount depends on the shape and the size of conductive particles and the target of the application. [25] Typically the size of conductive particles is 5 – 50 µm [29]. The most common materials of the conductive particles are gold plated nickel and metal plated polymer [25].

There are two types of ACA: anisotropic conductive film (ACF) and anisotropic conductive paste (ACP). The films and the pastes have differences in the bonding process

and the needed equipment. Typically, ACFs are supplied in reels and the film only needs to be cut of a suitable size and placed on the substrate. As for ACPs, they can be applied either by printing or by dispensing with a syringe. Although ACFs require special machines and ACPs are cheaper, ACFs have several other advantages over ACPs. With ACP, the amount of conductive particles in the connection is difficult to evaluate and it may lead to the quality problems of the connections. With ACF, it is possible to use a smaller size of a pitch. However, the size of the conductive particle needs to be considered when the pitch is smaller. In addition, the material consumption in the process is lower with the film than with the paste. [25][29][30]

The bonding process of the ACF starts by cutting the film to the correct size. After that, the film is placed on the substrate. It has to cover the entire bonding area. Pre-bonding is implemented by using low temperature and light pressure. Then, the carrier film is removed from the ACF. Next a component is picked and aligned. The component is pressed onto the adhesive and at the same time heat is applied on the component. As the temperature is raised, the adhesive transforms into low viscosity fluid. Then some of the conductive particles are trapped between the pads of the component and of the substrate. These particles form the electrical connections that conduct only on z-direction. [25] The adhesive also fills all the spaces around the contacts and provides both insulation in x-y-directions and mechanical support for the formed connections. The ACF bonding process is illustrated in Figure 7. The ACP does not need pre-bonding so the steps a and b in Figure 7 are replaced by the deposition of the ACP. However, the steps c and d of Figure 7 are performed similar as with the ACF.

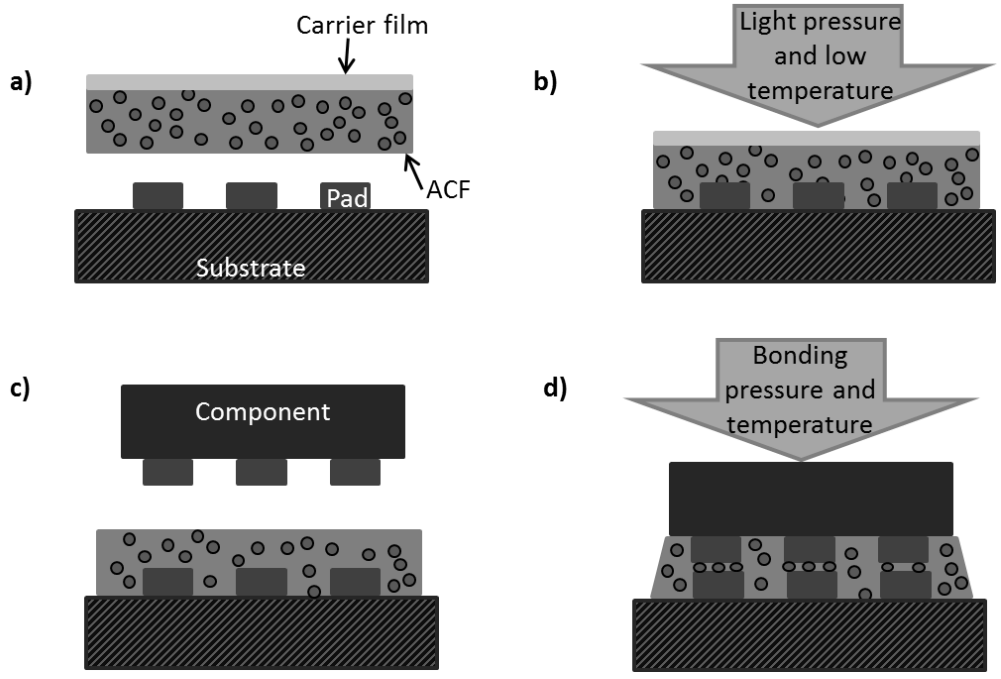

Figure 7. *A schematic illustration of the ACF bonding process: a) the ACF placement on the substrate, b) the pre-bonding, c) the alignment of the component to the substrate and d) the final bonding.*

The ACA joint has several advantages compared to the solder joint. The ACA attachment process does not need flux or cleaning. The process does not have lead emission due to the solderless process. In addition, the polymer matrix provides the mechanical support for the contacts thus no underfill is needed. That is an advantage also when compared with the ICA bonding process. Fewer process steps make the fabrication process cheaper. Because of the operational mode of the ACAs, they can be used in very high density applications. As an adhesive one, the ACA does not need high temperatures, which makes it compatible with the polymer substrates. On the other hand, the ACA does not have self-alignment capability, which has to be taken into account in the bonding process. A bonding machine has to also provide heat and pressure continuously during the attachment process. In addition, the final ACA joints have lower current capability and higher contact resistance than solder joints. [25]

The applied bonding conditions, temperature and pressure, are critical parameters for the optimal curing process of the ACF. The applied bonding temperature affects strongly on the adhesion strength because it directly correlates with the curing degree of the ACF. An increase in bonding temperature makes the chemical bonding stronger and the adhesion strength at the ACF interface better. In addition, high temperature lowers the surface energy of the ACF resulting wetting and flowing of the ACF. However, too high bonding temperature may increase the brittleness of the ACF and reduce its stability. [31]

As for the bonding pressure, it is used to compress the conductive particles against the conductive parts. With that effect, the adhesion strength of the ACF joints can be controlled. However, an increase in pressure increases the bonding strength only slightly. With the pressure, the thickness of the adhesive can be controlled which have an effect on the adhesion. However, an excessive pressure may cause an unreasonable deformation of the core of the particles or cracks in the metal layers of the conductive particles. The cracking causes large mechanical stress around the particles which may cause delamination or cracking in the contact areas. In addition, the overly high pressure can lead to high compressive stress or internal stress on the adhesive. When the stored elastic compression is releasing, it may cause a loss of the contacts. [31]

In this thesis, several anisotropic conductive films are used. In Table 2 is presented some properties of them. Temperature, time and pressure are the critical parameters of the final bonding and they affect strongly on the quality and the reliability of the joints. In a laboratory pre-bonding pressure and temperature can typically be applied by a hand. After that, the liner can be removed by using a pair of tweezers.

Table 2. *Conductive filler, pre-bonding properties and bonding properties of the ACFs used in this thesis* [32][33][34]

Item		**tesa HAF 8414**	**3M 7303**	**3M 9703**
Conductive filler	**Type**	NA	Ag-coated glass	Ag/Ni
	Diameter (µm)	40	43	NA
Adhesive Thickness (µm)		~10	74	50
Liner Thickness (µm)		~80	100	100
Pre-bonding	**Temperature (ºC)**	130 – 150	25 – 30	NA
	Time (s)	1.5 – 3.0	~1	NA
	Pressure (bar)	4 – 6	1 – 15	NA
Final bonding	**Temperature (ºC)**	160 – 180	140	15 – 70
	Time (s)	2.0 – 4.0	25	NA
	Pressure (bar)	15 – 35	>18	0.1 MPa

Because the softening ranges of Platilon and other substrates are relatively low, the bonding temperature is one of the key criteria when choosing the ACFs. Electrical conductive adhesive tape, 9703 by 3M, is a pressure sensitive adhesive (PSA) transfer ACF tape that can be bonded at the room temperature [34]. Both HAF 8414 by tesa and 7303 by 3M are heat-bondable ACFs but they can still be bonded in a relatively low temperature [32][33].

2.4.3 Non-Conductive Adhesive

A non-conductive adhesive is an insulator that holds the pads of the substrate and the pads of the component in contact. It also gives a mechanical backup for the connections. An illustration of NCA connection is presented in Figure 8. Although the NCA technology has been used mainly in the flip chip bonding process, there has been a study about applying that technology for the electronics in textiles [35].

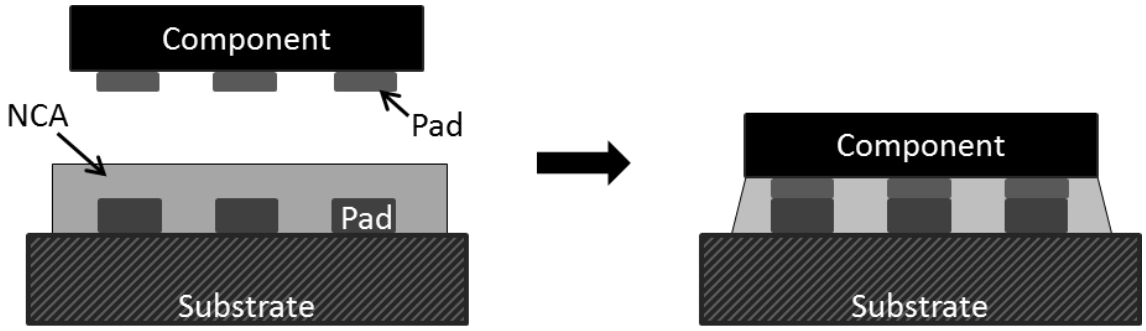

Figure 8. *A schematic illustration of NCA connection*

The NCA bonding process has fewer process steps in attachment and as an adhesive one it is more environmental friendly than solders. In addition, NCA has good compatibility with several materials. With NCA, the risk of shorts is very small so it can be used in applications with finer pitch than solders or other adhesives. [36] In this thesis, two NCAs by Permabond are used: ET515 and UV640. Curing properties and additional information about them are provided in Table 3.

Table 3. *Some properties of the NCAs* [37][38]

	Permabond ET515	**Permabond UV640**
Chemical composition	Epoxy resin	Methacrylate ester
Curing conditions	At 23 ºC, under pressure	UV LED 100mW/cm^2
Curing time	30 min	10 s (low power 4mW/cm^2 battery lamp)
Full cure	72 h	10 s (low power 4mW/cm^2 battery lamp)
Hardness of cured adhesive	30-50 Shore D	55-75 Shore D

ET515 is a two-component epoxy adhesive with good adhesion to a variety of substrates. It offers the full cure at the room temperature under pressure. Nevertheless, it requires rather long time for reaching the full cure. [37] Ultraviolet (UV) curable adhesive, UV640, has an excellent adhesion to plastics. In addition, the curing process of it can be implemented fast even with low-power lamps and it reaches the full cure immediately after the curing process. [38] Both adhesives by Permabond are an ideal in applications with different thermal expansion coefficients [37][38].

2.5 Fundamental Failure Mechanisms of Adhesive Connections

An adhesive creates a mechanical junction between two surfaces. The durability of the junction can be examined with adhesion and cohesion. The adhesion means the attractive forces between two different surfaces. [30] Insufficient adhesion causes fracture at the interface and the adhesive is totally or partially separated from the surface of the substrate. As for the Cohesion, it means the internal bond strength of the material [30]. Hence, the cohesion fracture can occur in both the adhesive and the substrate. In Figure 9, three typical fracture mechanisms of an adhesive joint are presented.

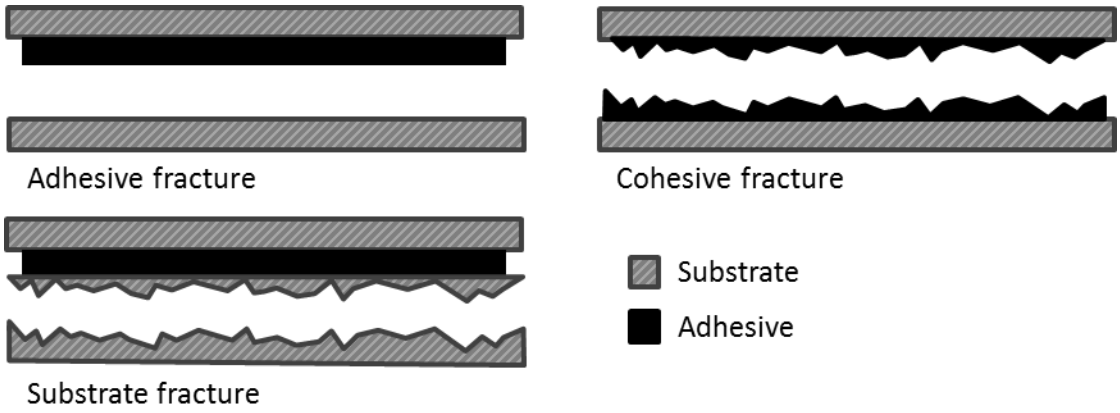

Figure 9. *Three fracture mechanisms of an adhesive joint*

A premature fracture of an adhesive joint can be prevented by choosing the correct adhesive, by the preparation of the adhesive junction point and by suitable adhesive junction designing. The cleaning of the surfaces with a solvent for example is an important preparation method. [30]

In electronics manufacturing processes, the adhesives introduce new opportunities for bonding on the stretchable substrates. On the other hand, they also lead to new challenges. Delamination at the interfaces and cracking at the contacts are typical failure mechanisms of adhesive connections made by common epoxy adhesives. These problems are typically caused by mechanical stress or moisture diffusion. In addition, oxidation and corrosion on the surfaces are typical failure mechanisms for many base metal contacts but they can be avoided by adding gold surfaces on the contacts. [39]

Epoxy resin adhesives with a high value of Young's Modulus are commonly used for bonding because they can achieve strong adhesion and cohesion with a substrate. However, the structure with the epoxy resin adhesive is rigid and together with temperature dependent motions, they cause high shearing forces. [39]

3. METHODS

The aim of this thesis is to execute and evaluate adhesive joints between printed stretchable interconnects and a rigid component. Test samples are manufactured in order to test the joints. One test sample consists of a stretchable substrate, stretchable interconnects, a rigid component and adhesive joints. The stretchable interconnects are manufactured by using a screen-printer. Although the quality of the printing process and the initial performance of the interconnects are also evaluated, the main focus in this thesis is on the component mounting. Various adhesives are investigated and tested with a strain test. Five samples with the same substrate and the adhesive combination for the tests are manufactured. In addition, another strain tester is designed, manufactured and evaluated.

3.1 Screen-Printing on Stretchable Substrate

In this thesis semi-automatic DEK 248 screen-printer is used for manufacturing the stretchable interconnects. The screen printer is shown in Figure 10. The interconnects are printed with silver ink, CI-1036 by ECM. Three TPUs are used as a substrate material: Platilon U4202 by Epurex Films, TPU1 and TPU2.

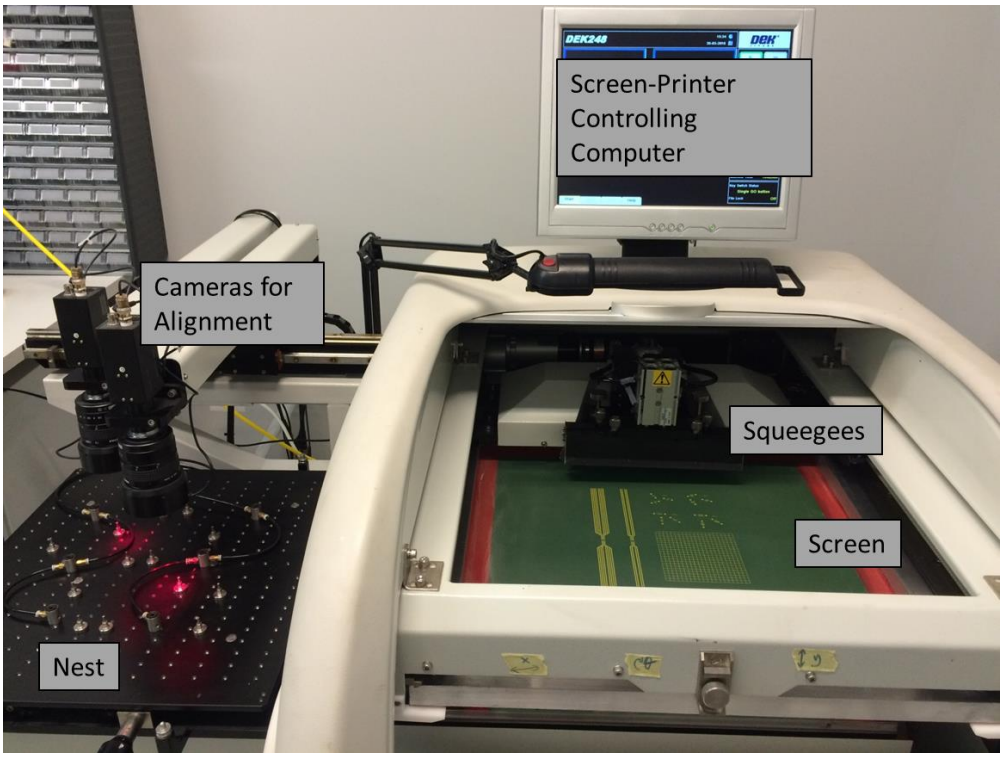

Figure 10. *The screen-printer, DEK 248*

In order to minimize the solvent loss and maximize the self-life of the ink, it needs to be stored under 15ºC. However before printing, the ink has to reach the room temperature and it needs to be gently stirred with a spatula for 1-2 minutes. These pre-steps are done in order to keep the rheology of the ink suitable for the screen-printing process. In addition, high velocity or a high shear mixer has to be avoided because they can induce air bubbles.

The screen-printer uses two single diamond squeegees. One of them sweeps from the back to front and the other one in the opposite direction. The material of the squeegees is rubber. The parameters of the screen are based on the information provided by the ink manufacturer and the dimension limits of both the screen-printer and the squeegees. The parameters of the screen are listed in Table 4.

Table 4. *The parameters of the screen*

Parameter	**Screen**
Mesh Material	Polyester
Frame Material	Aluminum
Frame Size (mm^2)	508 x 508
Mesh Thickness (µm)	79
Mesh Count (Threads/cm)	77
Mesh Angle (º)	22.5
Thread Thickness (µm)	55
Screen Tension (N/cm)	22.3

The manufacturing process of the screen-printing starts by cutting the substrates into pieces. Platilon U4202 is only 50µm thick and does not have carrier film which makes its handling demanding. Consequently, the samples of Platilon are pre-stretched slightly and attached to aluminum plates with tape. This is done in order to keep the substrate steady and flat during both the printing phase and the curing phase. The other two substrate materials, TPU1 and TPU2 are thicker and do not need pre-stretch. TPU1 also has the carrier film. However, in order to make the handling of them easier during the manufacturing process they are still attached to the aluminum plates with tape. The size of the aluminum plates is 300 x 150 x 2 mm^3.

One sample of the substrates at the time is placed on the nest that is on the left side of the screen-printer. The alignment of the substrate is done manually with the help of two cameras. The nest and the cameras can be seen in Figure 10. Before starting the printing process, the surface of the substrate is cleaned with isopropyl alcohol (IPA) in order to remove stains and dust that could impair the printing quality.

The preparation of the screen-printer starts by installing the screen and the squeegees to the printer. Next the ink is spread on the screen in the front of the farthest squeegee. The

printing parameters are set in the screen-printer controlling computer and only the squeegee pressure needs to be set manually. After that, the printing is automatic. When run is pressed, the nest moves into the screen printer and rises up. The printing is implemented by flood/print –order. So, first the farthest squeegee is settled on the screen. Then, both squeegees move forward but only farthest squeegee touches the screen and pushes the ink through the screen. When the squeegees reach the front print limit, they stop and wait for the time of the squeegee delay. After that, the farthest squeegee rises up whereas the front squeegee is settled on the screen. Now they are moving backward and the front squeegee pushes the ink through the screen. Again, they stop when they reach the rear print limit. After that, the nest goes down and moves back to its original place. The pattern is now printed on the substrate and the printing quality can be reviewed. If the quality is insufficient, the optimal printing parameters are searched by printing with different combinations of the parameters. The printing can be done on the aluminum plate without attaching the TPU because the plate can be easily cleaned with acetone between the printings. The printing parameters that are used in this thesis are listed in Table 5. There deposits -parameter describes the cycles of flood/print –phase. With more cycles, it is more probable that all holes are filled with the ink. On the other hand, an increase of the cycles also increases the risk that the ink floods, which makes the print quality again insufficient.

Table 5. *The printing parameters of DEK 248*

Property	**DEK 248**
Deposits	2
Forward Speed (mm/s)	50
Print Speed Backward (mm/s)	70
Print Gap (mm)	1.0
Front Print Limit (mm)	50
Rear Print Limit (mm)	380
Separation Speed (%)	50
Table In Delay (s)	2.0
Squeegee Delay (s)	5.0
Squeegee Pressure (kg)	14.5

In order to make the printed patterns conductive, they need to be cured. According to the datasheet of the ink, the typical forced curing is 10 minutes at 120 ºC [22]. However, the aluminum plates under the TPUs affect the curing process. In Jari Suikkola's thesis, the suitable curing schedule was found to be 30 minutes at 125 ºC, so the same schedule is used in this thesis [40].

A printed test pattern is presented in Figure 11. In the middle of the pattern, the line width is 0.71 mm and in the other parts it is 1.2 mm. The minimum gap width is 0.6

mm. The total length of the pattern is 26 cm and the thickness is 1.86 cm. After curing, the samples are cut to desired shapes. In this thesis, both of the test setups require the different shape of the sample.

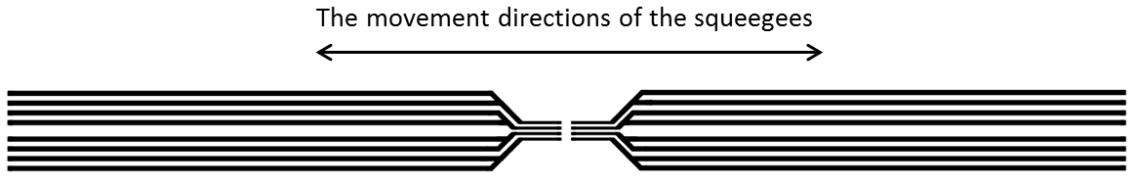

Figure 11. *The printed test pattern for the strain tests. The size of the pattern is 26 x 1.86 mm^2. The minimum line width is 0.71 mm and the minimum gap width is 0.6 mm.*

The test pattern is designed to support 4-point resistance measuring when a resistor array is mounted in the middle of the pattern. The value of the used resistor array is 100 Ω ± 1 Ω. The 4-point resistant measurement is used in this thesis in order to focus on the electrical resistance changes more in the adhesive joints and less in the printed interconnects.

3.2 Component Mounting on the Substrate

The component mounting is implemented by three types of adhesives: isotropic conductive adhesive, anisotropic conductive adhesive and non-conductive adhesive. Common to all mounting methods with adhesives is that the substrate needs to be clean and dry. So, once again the surface is cleaned carefully with IPA and all the stains and dust are removed in order to improve the quality of the mounting process and the adhesive joints. However, every type of the adhesives requires different circumstances and methods in the curing process.

3.2.1 Isotropic Conductive Adhesive with Underfill

In this thesis, silver epoxy adhesive, DB-1561 by ECM is used as an ICA. The underfill, UF-9526 by ECM, is a non-conductive attachment adhesive that is used to assist the ICA. The underfill needs to be stored under 0 ºC whereas the ICA is stored under 4 ºC. Both the ICA and the underfill are two-component systems and before they can be mixed, they have to reach the room temperature.

The dispensing of the ICA and the underfill is done by a needle. Firstly, the ICA is applied on the pads. After that, the underfill is applied between the pads. The component needs to be placed carefully because of the lack of self-alignment properties. The forced curing is implemented at 70 ºC for 40 minutes. During the curing process, also pressure needs to be applied to the joint in order to prevent the rise of the component.

3.2.2 Anisotropic Conductive Adhesive

The ACAs need a special equipment in order to provide both pressure and heat at the same time for a specific time. The parameters of the process depend strongly on the adhesive. On the other hand, the used equipment may set limits for the parameters. Two manufacturing systems for the ACF bonding process are studied. A heat press is presented in Figure 12 and Finetech Fineplacer later in Figure 13. In both manners, the prebonding is done by hand and the carrier film is removed with a pair of tweezers.

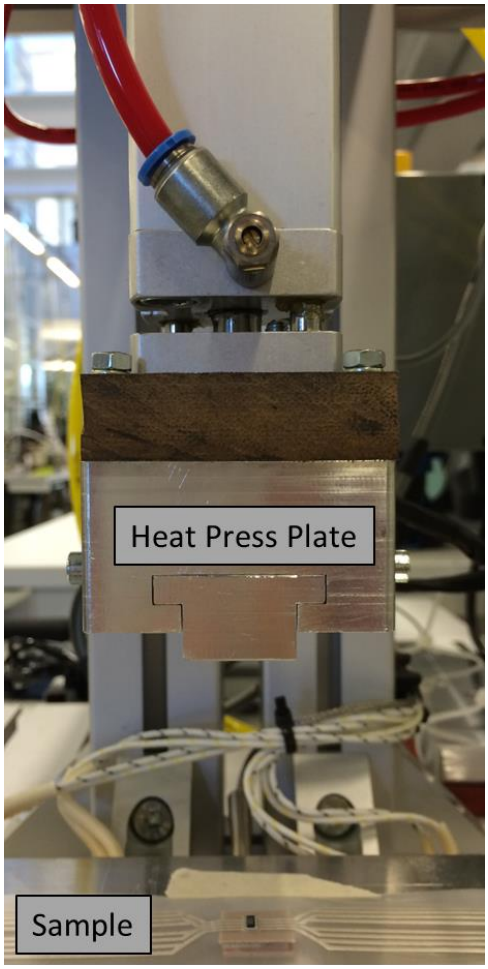

Figure 12. *The heat press for the ACF bonding processes*

The bonding process with the heat press starts by setting the parameters: temperature, pressure and time. Then the heat press plate heats to the bonding temperature. After that the sample is placed at the point on the place that is direct under the heat press plate. Lastly, the heat press plate is settled down. When the bonding time has passed, the press plate rises up automatically.

In the bonding process with the heat press, the suitable parameters for each ACF were first determined with the help of a rigid PCB with a copper surface. The adhesive was cut and placed on the PCB and the component on the top of the adhesive. Then the bonding process was implemented by the heat-press. After each bonding the contacts

were checked. If all the contacts were not formed, the bonding parameters were set again. In case of all the contacts were formed, the bonding was implemented again with the same parameters in order to ensure that it was not just a coincidence. When the sufficient parameters were found for each ACFs, the same parameters were used also in the bonding process with the different TPU materials. However, the same parameters that were used to connect the component to the rigid substrate successfully did not form the contacts when the component was mounted on the stretchable substrate.

With some improvements in the bonding process, some contacts could be formed randomly. A problem that occurs with TPUs was that when the heat press plate was settled down, the component might have stirred. However, with a small piece of silicon under the substrate, the stir could be prevented. Because the used temperatures are quite high for the TPUs, a piece of teflon was used in the top of the component in order to prevent the substrate from grapping the heat press plate. With these improvements, the contacts were able to be formed with the ACF by tesa. Then the temperature of the plate was 150 ºC and the bonding time 20 seconds. The pressure of the heat press was 1.4 bar. The corresponding pressure that is applied to the ACF can be calculated. The pressure is expressed as

$$p = \frac{F}{A}, \tag{5}$$

where F represents force that is applied to the surface of an object and A represents the area of the surface. The force generated by the heat press equals the force that is applied to the surface, so

$$p_1 * A_1 = p_2 * A_2. \tag{6}$$

There p_1 represents the pressure of the heat-press, A_1 is the area of the piston, p_2 is the pressure applied to the adhesive and A_2 is the area of the component. So, the pressure that is applied to the adhesive is

$$p_2 = \frac{p_1 A_1}{A_2}. \tag{7}$$

By using Equation (7), the applied pressure to the ACF is calculated to be 10.6 bar.

The other equipment that is studied for the ACF bonding process is Fineplacer that is presented in Figure 13. The attachment process with Fineplacer starts by cutting the ACF and placing it on the substrate that has the printed interconnects. After that, the pre-bonding is done. Next, the component is picked up with the tool. Then the substrate with the ACF is placed on the plate of Finaplacer. The alignment is done manually by moving the plate. The correct place for the plate can be found because both of the attached surfaces can be seen at the same time in the microscope. The parameters of the bonding process are set on the controlling computer. The heat can be set on both the

tool and the plate. Also, the bonding time is set. The pressure is set manually by moving a weight that is attached to the tool. The weight can be chosen between 0.1 – 20 N. After the parameters are set, the tool is laid down and the component is pressed against the ACF that had been placed on the substrate. Then the heating is started and when the bonding time is elapsed, the tool is lifted up and the joints should be created.

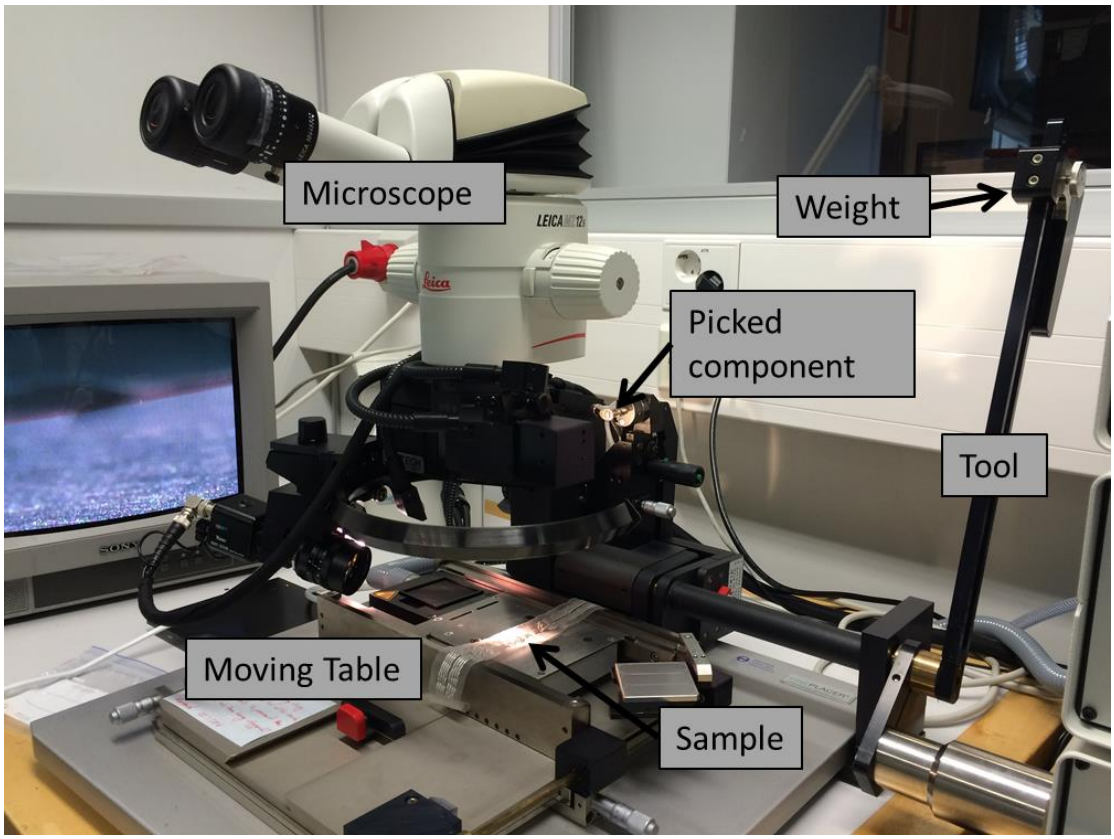

Figure 13. *Fineplacer for the ACF bonding process*

Fineplacer was used in the 3M ACF 7303 bonding process. The sufficient bonding parameters were found so that right after the process the contacts were formed. However, when the contacts were explored again after a day, some contacts were lost. The bonding process was repeated on another day and the same phenomenon occurred. The reason for the phenomenon was not further inspected within the framework of this thesis. Consequently in the Future, the ACF would need additional researching in order to create sustainable joints between the component and the TPU.

The conductive tape, 9703 by 3M, should not need extra heat in the bonding process but it formed insufficient connections in the room temperature. Under the pressure, the connections were formed but when the pressure was removed some or all of the contacts were lost. The bonding process was implemented with both the heat press and Fineplacer but the same effect appeared as in the room temperature. So, also the conductive tape would need further research and it is not done in this thesis.

Because the stretchable electronics technology is a quite new technology area, there are not commonly available ACFs that would be meant for rigid to stretchable connections. The ACFs in this thesis are meant to rigid to flexible connections and the bonding parameters that were given in the datasheets of the ACFs are meant for connections like that. When connecting the resistor array to the stretchable substrate, there are also other properties that need to be taken account when giving the bonding parameters. The component is a passive component that has pure thin solder contacts that may permit under the pressure and the heat. That might be the reason for the phenomenon which occurred with the conductive tape, 9703. On the other hand, the used TPU materials are soft and their softening temperatures are relatively low. So, they might also permit and transform during the bonding process which affects the quality of the joints. In addition, the heat press plate introduces other challenges because it is at a little angle therefore the pressure does not distribute uniformly on the plate. So, the component needs to be placed in the certain point in order to achieve uniformly distributed pressure.

3.2.3 Non-Conductive Adhesive

Both two NCAs used in this thesis, require totally different curing circumstances. ET515 needs pressure but the curing can be implemented in the room temperature. On the other hand, UV640 requires UV-light to be cured.

As a two-part epoxy adhesive, ET515 is stored in a dual cartridge. So, it can easily be mixed with an application gun and a static mixer. Firstly, the cartridge is inserted into the application gun and the plunger of the application gun is guided into the cartridge. Next, the cap of the cartridge is removed and materials are dispensed until both sides of the cartridge are flowing. Then, the static mixer is applied to the end of the cartridge and the dispensing of the adhesive can begin. In Figure 14, the structure of the system is illustrated. The adhesive is applied to the substrate and the component is placed on top of it. In the end, the assembly needs to be clamped in order to provide required pressure for 30 minutes or until handling strength is obtained. In addition, the joints need 72 hours to reach the full cure. [37]

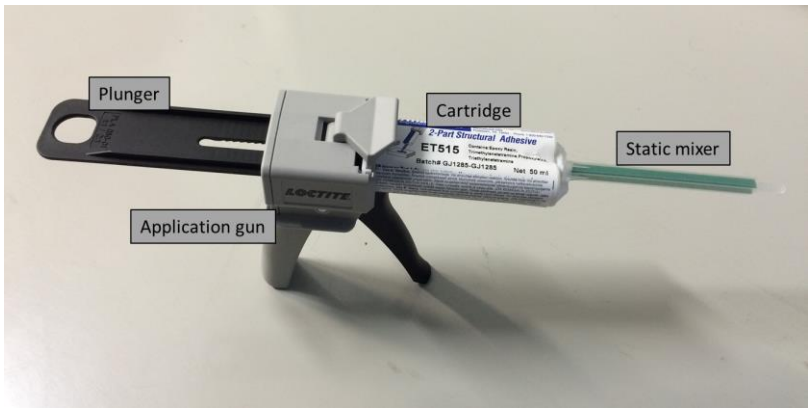

Figure 14. *The adhesive cartridge applied to the application gun*

The device for the UV-curing process is made for this thesis and it is presented in Figure 15. UV-curable adhesives require UV-light with a special wavelength. In case of UV640, the wavelength of a light source has to be between 365 nm and 420 nm. The chosen UV-LEDs by OSA Opto Light have a wavelength between 390 nm and 395 nm [41]. In addition to eight UV-LEDs the curing device includes a switch and a battery of 4.5V. The UV-curing system is designed so that the component is surrounded by the UV-LEDs during the curing process.

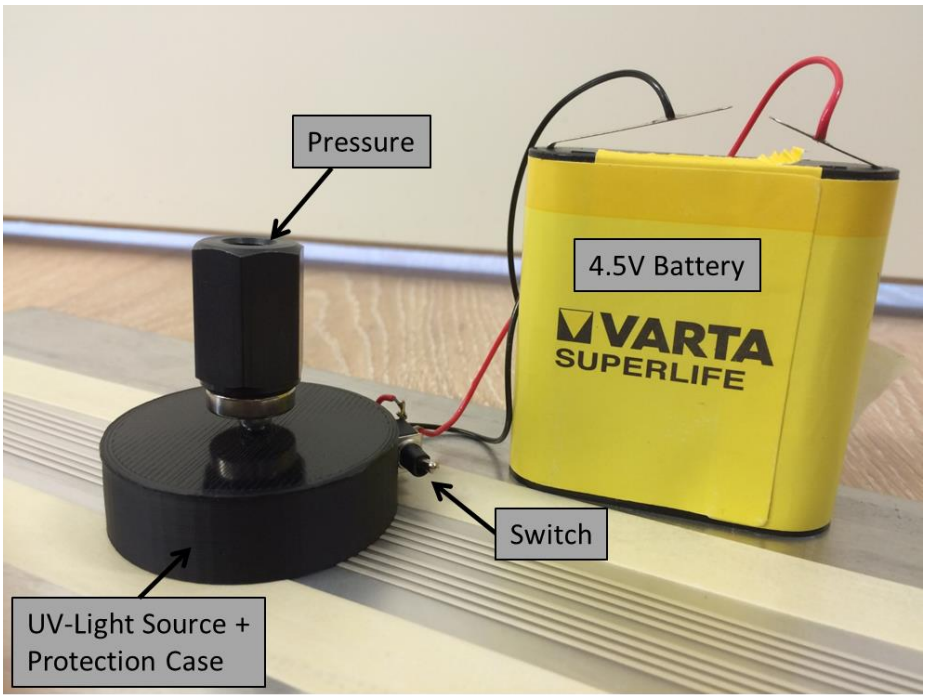

Figure 15. *The UV-curing system*

The NCA UV-curing process starts by applying two little drops of the adhesive on the substrate. The component is carefully placed on the top of the adhesive due to the lack of a self-alignment property. In addition, a little pressure needs to be carefully applied to the component before and during the UV-curing process in order to get the adhesive move over so that the electrical contacts can be formed. The sufficient exposing time was found by exposing the joints to the UV-light in 10 second cycles. After every cycle, the hardness of the adhesive was inspected. When the sufficient hardness was obtained, no additional exposing cycle was required. The exposing time was found to be 90 seconds.

3.3 Sheet Resistance

The initial electrical properties of the screen-printed ink are inspected by measuring the resistance of the printed interconnects. Resistance of a three-dimensional system is defined

$$R = \rho \frac{L}{Wt}, \tag{8}$$

where ρ represents the resistivity of the conductor, L is the length of the conductor, W is the width of the conductor and t is the thickness of the conductor. However, for a thin-film application the thickness may be complex to define and the variations in the thickness can be significant in comparison of the total thickness of the conductor. So, in order to evaluate the electrical properties of a thin-film application, sheet resistance is used and it can be defined

$$R_S = \frac{\rho}{t}. \tag{9}$$

With the sheet resistance, the electrical resistivity can be defined without taking the thickness of a conductor into account. By combining Equation (8) with Equation (9), the sheet resistance can be calculated as

$$R_S = R \frac{W}{L}. \tag{10}$$

The unit of the sheet resistance is Ω/□. Typically, a Greek cross structure is used in defining the resistance. That structure is illustrated in Figure 16. The structure supports 4-point resistance measuring when the contact resistances are avoided. [42]

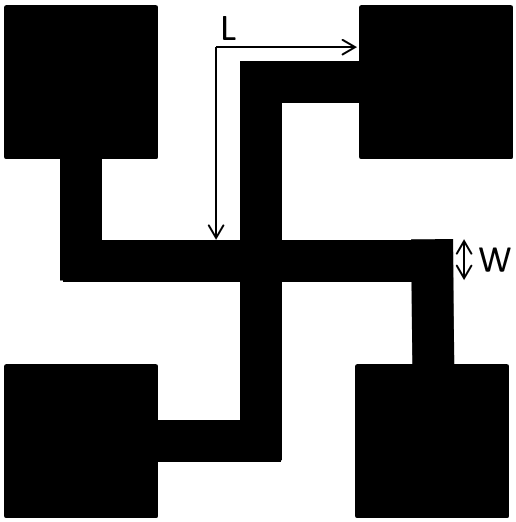

Figure 16. *A Greek cross structure*

However, in this thesis, 2-point resistance measuring is used to determine the sheet resistances of the interconnects. Thus, the measurements include also the contact resistances but they are reduced from the measured resistance values. Resistances are measured by Fluke 183 True RMS Multimeter which contact resistance is 0.2 Ω. The sheet resistances of the thicker parts are almost two times greater than the sheet resistances of the thinner parts of the interconnects. So, the sheet resistances are defined only for the thicker parts.

3.4 Test Setups

In this thesis two strain tests are explored. The most common and simplest stretching manner, the uniaxial stretch is used in a cyclic stretching test. The evaluation of the electrical performance is implemented by measuring the changes of the electrical resistance during the stretching with the 4-point resistance measuring. In addition, a custom-made test setup is designed and manufactured for this thesis. The setup differs from the other setup by stretching the sample in every direction. The properties of that setup are evaluated by comparing it with the uniaxial stretching. The one-time stretch test method is used in the comparison. In that method, the sample is stretched until the connections are lost.

3.4.1 Tinius Olsen H5KT Benchtop Tester – Based Setup

Tinius Olsen H5KT Benchtop Tester – based setup is used for cyclic stretching testing. The setup is shown in Figure 17. The setup includes four resistance measurement devices that enable the 4-point resistance measuring. In addition, two computers are used for controlling the strain test and saving the resistance measurements.

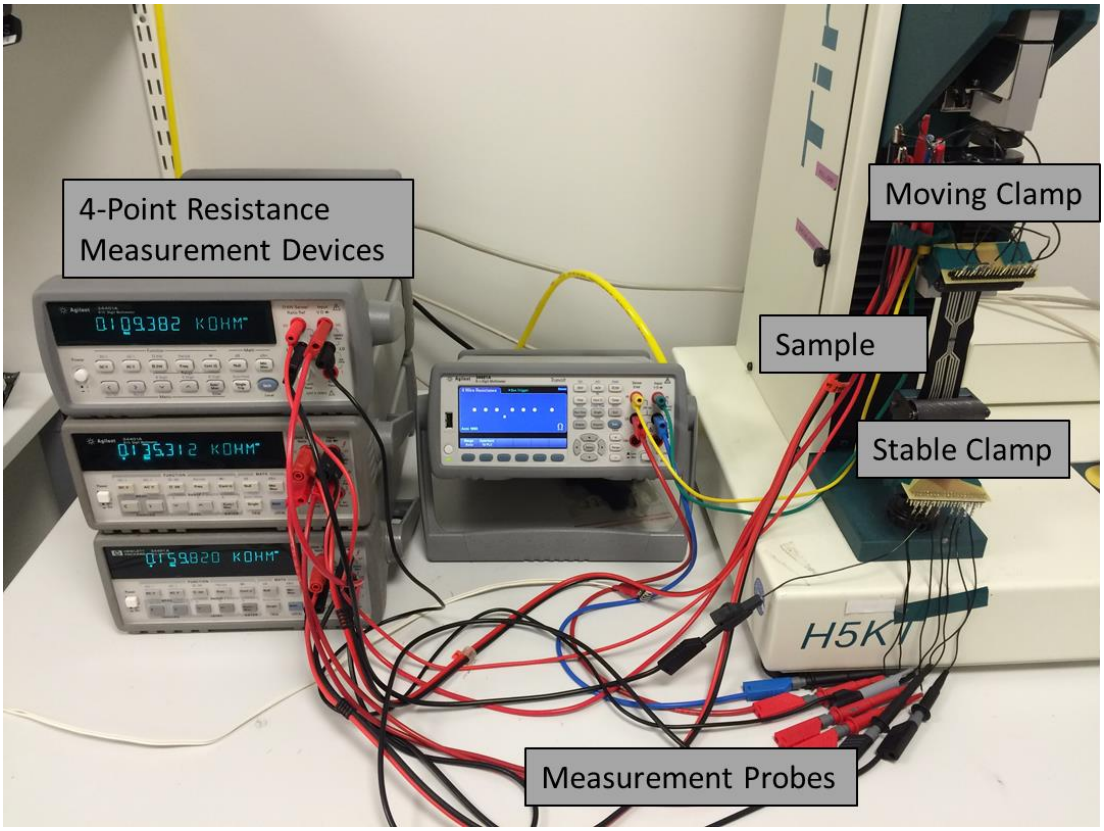

Figure 17. *Tinius Olsen H5KT Benchtop Tester –based setup*

The preparation of the strain test starts by adjusting the distance between the clamps. The upper clamp is moving and the lower clamp is a static one. The clamps are metallic

and their surfaces are rough, therefore parts of the samples are protected with double-sided tape. The tape also prevents the slipping of the sample when it is stretched. Another challenge in this setup is to create the connection from the stretchable interconnects to the rigid resistance measuring probes. Firstly, the ends of the interconnects are reinforced by a PVC based film and connected to a board connector. Then, the board connector is connected to a pin header by way of a rigid PCB. Lastly, wires with female contacts are used to connect the resistance measuring wires to the pin header.

With the strain test controlling computer, the parameters for the cyclic stretching test can be set. Before starting the testing, the calibration of the setup is done. The forces caused by the weight of the attached sample are reduced from the measurement. Also, the extension needs to be zeroed before starting the testing. After every cycle set, the program also presents the proportionality between the force and the extension. The resistance measurement logging is done by Benchvue by Keysight Technologies.

3.4.2 Custom-Made Test Setup

The custom-made test setup is designed and manufactured for this thesis. The test setup is designed to stretch the substrate for the same amount in every direction at the same time. In that way, the stretching situation is planned to correspond a real life stretching situation. The structure of the setup is presented in Figure 18.

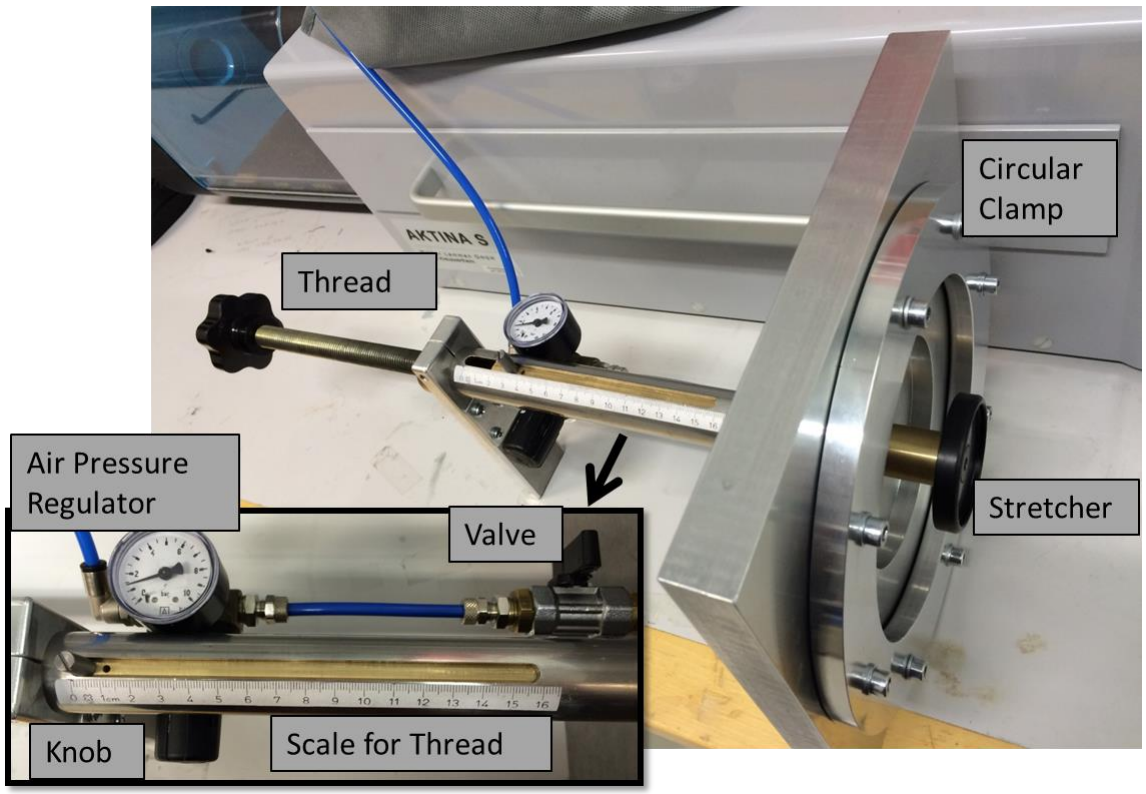

Figure 18. *The structure of the custom-made test setup*

A test sample is circularly clamped to the setup. The sample stays still under the clamp by way of an O-ring seal. In addition, the clamp is fastened with eight bolts. The screwing of the thread causes a movement in the stretcher. However, the friction between the plastic stretcher and the sample affects the stretching situation strongly. The friction can be decreased for example by compressed air or lubricant. Because the compressed air also has another advantage, it is used in this thesis. The advantage can be seen from Figure 19 where the stretching of the substrate is demonstrated without and with the compressed air. In both situations, the stretching is constant in every direction in the middle of the stretcher. However, the compressed air improves the steadiness of stretching on the sides of the stretcher.

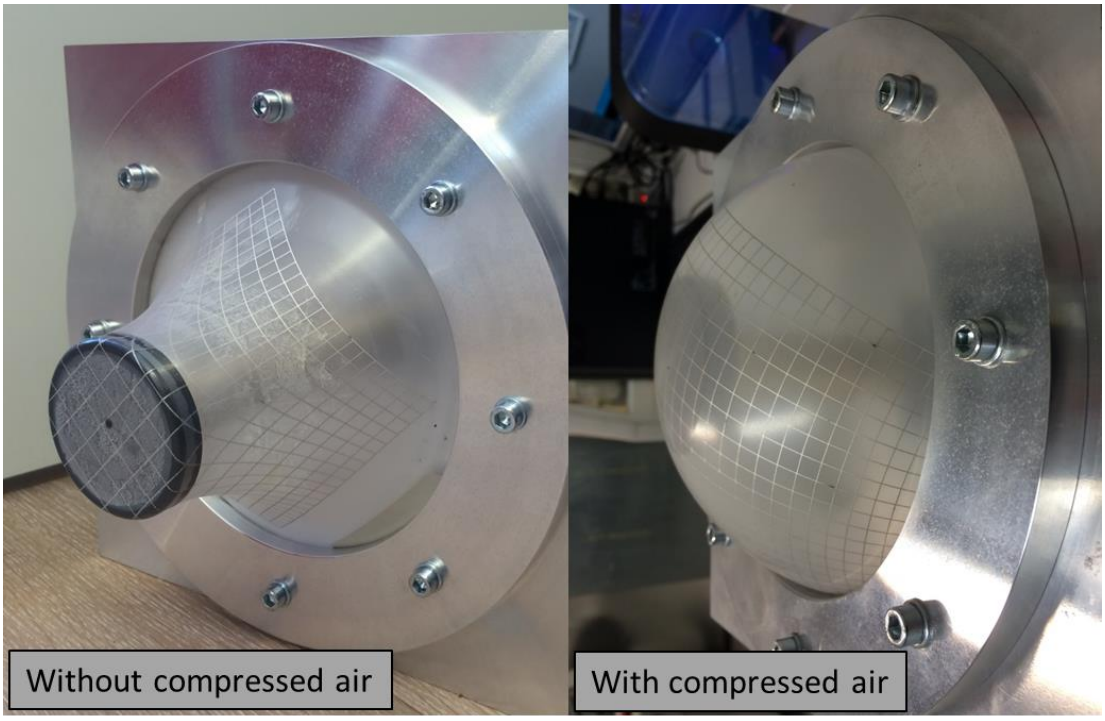

Figure 19. *The grid-patterned sample in custom-made test setup without and with compressed air*

Before stretching the actual test samples, a grid –pattern is printed on three pieces of each substrate. With the grid –pattern, the manner of stretching is evaluated. For each TPU material, the proportions of the strain to the thread are presented in Figure 20. During the stretching, also compressed air needs to be added so that the friction cannot be increased too much. The increases in the compressed air can be seen as more constant area in Figure 20, for example around the strain of 50 %.

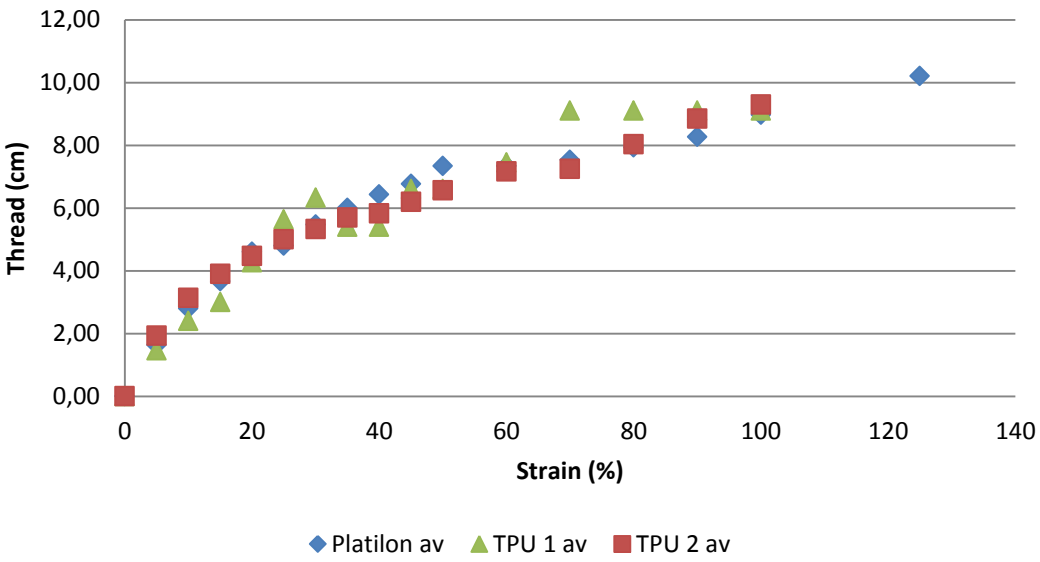

Figure 20. *The proportion of the strain of the thread and the strain of the substrate*

The test setup for the actual one-time elasticity test is shown in Figure 21. The setup also includes four resistance measurement units like the H5KT –based setup and Benchvue by Keysight Technologies is used to log the resistances. The connections between the stretchable interconnects and the rigid resistance measuring probes are done in the same way as with the other setup with the help of little circuit plates.

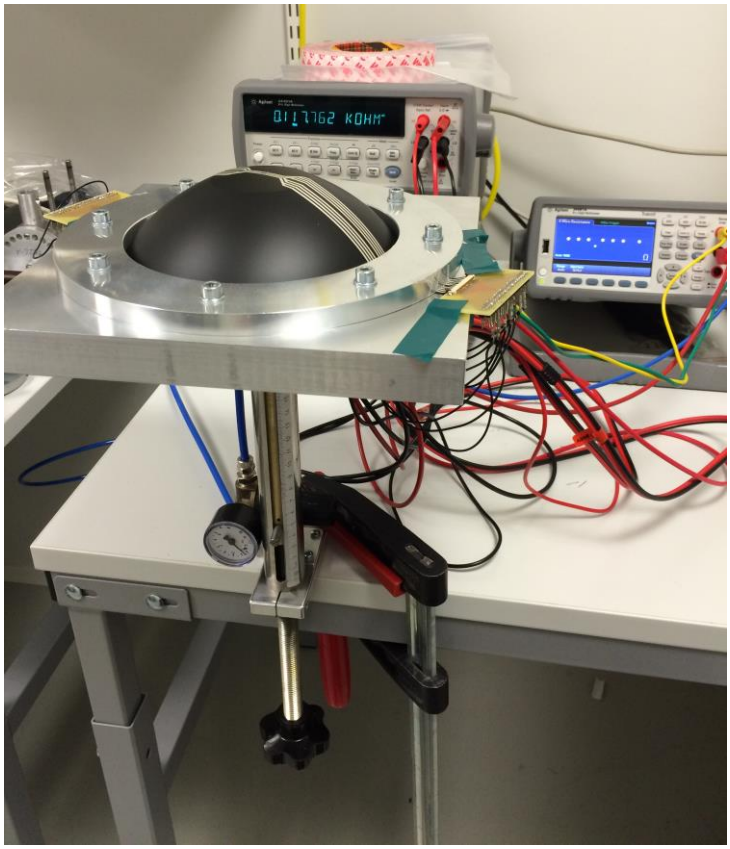

Figure 21. *The custom-made test setup with an actual sample*

The growth of compressed air and the movement of the stretcher are implemented always in the same order and with the same amount. Those are determined by way of Figure 20 but they are further modified so that they are more suitable for the actual patterned samples. The compressed air causes the substrate to curves also under the component which increases the stress on the surface between the substrate and the adhesive. Thus, when the compressed air was increased, also the stretcher needed to be moved up, in order to keep the curvature as small as possible.

3.5 Electromechanical Measurements

In this thesis, the resistances of all four channels are measured by using the 4-point resistance measurement. That is illustrated in the circuit diagram of Figure 22.

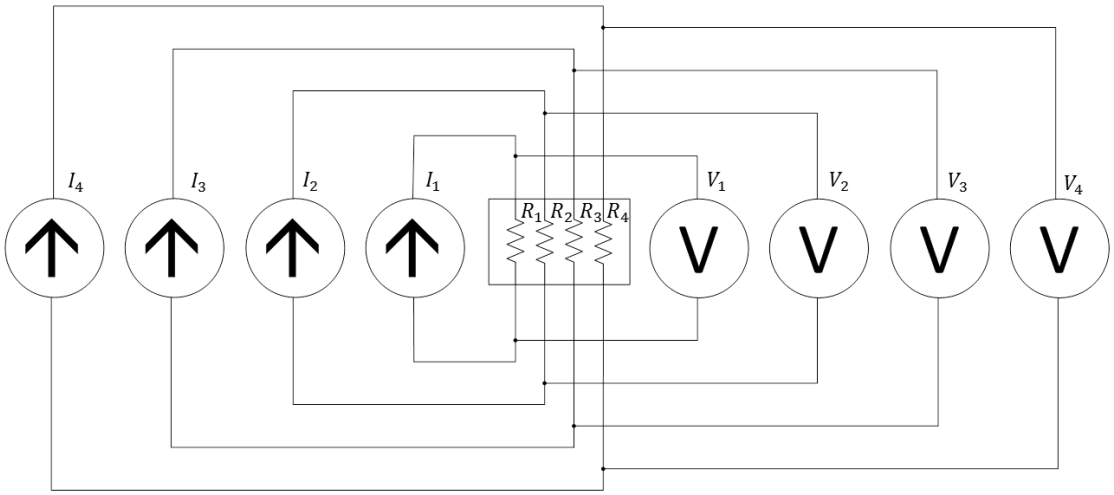

Figure 22. *The 4-point resistance measuring of the resistor array*

In addition to the resistance of the adhesive joint and of the component, all channels include parts of the resistances of the printed wires. However, significant parts of the wire resistances are removed by connecting the measurement probes as they are shown in Figure 23. Both ends of the wires are connected at the same way.

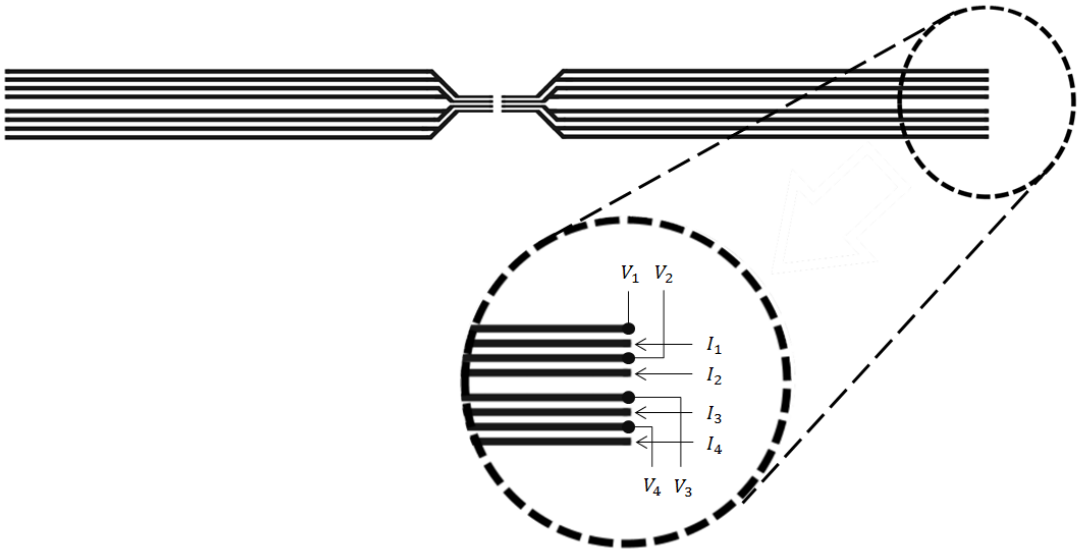

Figure 23. *The measurement channels of the printed structure*

In this thesis, the first test for evaluating the electromechanical performance of the adhesive joints is a cyclic strain test. Five samples of every combination of the substrate and the adhesive are manufactured for the test. Each test sample is cut to a size of 30 x 255 mm^2.

The cyclic strain test is implemented by the Tinius Olsen H5KT Benchtop Tester –based setup. The sample is attached under the clamps so that the extension range is 100 mm. The samples are stretched 10 % for 500 times. The used stretch rate is 200 mm/min. The resistances of the sample are continuously measured during the strain test. Although some connections of the sample might break during the stretching, the test is still not stopped before all the cycles are done. So, it can be figured out if the connectivity is lost only temporality. In addition, the measurement is continued 10 minutes after the last cycle, in order to monitor the changes in resistances immediately after the strain test. In addition, the resistances are measured once again after more than a day. The idea is that the substrate has time to return to its original shape before measuring.

The other strain test that is implemented in this thesis is the one-time elasticity test. Based on the cyclic stretching test, only the best combination of the adhesive and the substrate is chosen for that test. It is implemented with both H5KT –based setup and the custom-made test setup. The other aim of that test is to compare the results of the test setups and that way evaluate the performance of the custom-made test setup.

The pattern of the samples is the same in both test setups and it can be seen in Figure 23. However, the custom-made test setup requires that the sample is circularly formulated except at the points of the interconnects that are outside of the clamp. The diameter of the circle is 195 mm. The size of two outer parts is 30 x 30 mm^2. The sample is placed in the setup so that the resistor array is in the middle of the stretcher. Thus, it is

ensured that the stretching is as constant as possible in every direction. In addition, the aluminum parts of the tester that are in direct contact with the interconnects needs to be covered with tape so that they do not affect the measuring results.

The stretching parameters of H5KT in the one-time stretch test differ from the parameters that are used in the cyclic stretching test. In order to make the setups more comparable, the extension range is raised to 140 mm. In addition, the stretch rate of H5KT is reduced to the rate of 20 mm/min. The resistances of the sample are measured continuously during the stretching and they are monitored in real time. So, when some connection of the channels is lost, the extension point is marked up. After the last connection is lost, the samples are stretched approximately five percentage points more to ensure that the conductivity is not lost only temporarily.

With custom-made test setup, the determining of the extension is more complicated because the stretching occurs in every direction. So, before stretching the sample, two marks are drawn near to the component on the substrate. The distance between the marks is approximate 4 mm and the exact value is measured before the test. During the test, when a connection is lost the distance is measured again and it is compared with the initial distance. Thus, the measured extensions are uniaxial with both test setups and they can be compared.

4. RESULTS AND DISCUSSION

The results of the experiments and test-setups are presented and discussed in this chapter. For the cyclic strain test, five samples of each adhesive and substrate combination were manufactured. First, the initial electrical performance of the stretchable interconnects and the adhesive joints are evaluated. Then, the electrical performances of the joints under strain tests are discussed and compared with the results of the initial performance of the joints. In addition, the performance of the custom-made test setup is evaluated and compared with Tinius Olsen H5KT Benchtop Tester – based setup. Based on the cyclic test, five samples of the best adhesive and substrate combination for both setups are manufactured. At one time, the one-time stretch of the best combination is also explored.

4.1 The Quality of the Screen-Printed Interconnects

The quality of the screen-printed interconnects was roughly evaluated. Based on the evaluation two main quality issues were found.

The environment strongly influences the quality of the printed interconnects. The screen-printer is located into an electronics workshop that is not particularly clean. Although, the samples were cleaned before printing, there might still have remained some dust on the substrate. After the curing of the ink, the impurities became visible and looked like burned points. An example of them is shown in Figure 24. On the other hand, the screen-printer and the heating chamber are located in different rooms which might also increase the amount of the impurities during the transport and reduce the quality of the printed samples. These quality issues with the impurities could be removed by locating the machines in a clean room.

Figure 24. *Impurities on the printed interconnects*

Another significant printing quality issue appeared only with Platilon. The printed interconnects seemed to be good after the printing and the curing process. However, when a sample was stretched even slightly, the thinner part of the printed interconnects started to crack. The cracking also meant a loss of the connection. The same printing parameters were also used with the other TPUs and no cracking occurred during the stretching. Even though the printing parameters were modified several times, the cracking appeared. Either a stronger or a lighter pre-stretch of the sample did not fix the problem. In the research made before, the same ink and the same TPU have been used and no cracking was found. So, the main differences between the successful and unsuccessful printing are the screen-printer and the printed patterns. With the other screen-printer, the printing parameters need to be set manually so the comparison of the parameters cannot be directly done. Nevertheless, this thesis did not focus on that issue more but on the successful samples with other TPU materials.

4.2 Initial Electrical Performance of the Stretchable Interconnects

Because the main focus in this thesis is in the adhesive joints, the printed interconnects are designed relatively thick and they are expected to withstand the tests without breaking. So, before the component mounting, the interconnects were evaluated. The electrical resistances of the interconnects were measured in order to define the sheet resistances. In Figure 25 is presented the distribution of the sheet resistances for the substrates.

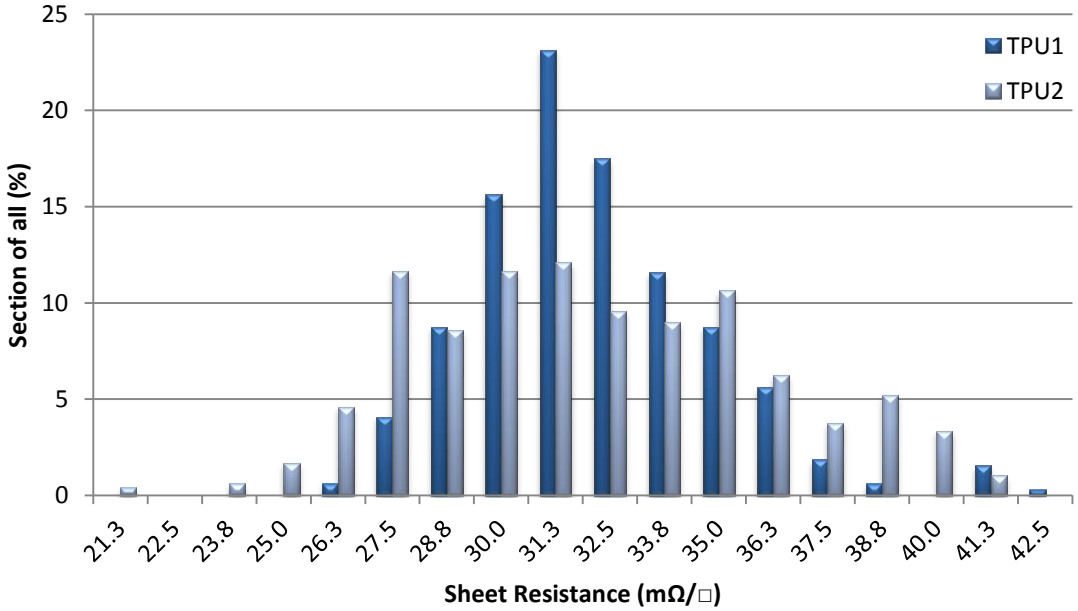

Figure 25. *The sheet resistances of the printed interconnects on TPU1 and on TPU2*

The average sheet resistance of the printed interconnects is 32.1 $m\Omega/\square$ for both of the substrates. However, the standard deviation of the sheet resistances is 2.72 $m\Omega/\square$ for

TPU1 while it is 3.99 $m\Omega/\square$ for TPU2. In the datasheet of the ink, the sheet resistance is reported to be lower than 10 $m\Omega/\square$ [22]. So, the measured sheet resistance values are systematically higher than in the datasheet of the ink is reported. However, this was not studied further in this thesis because the sheet resistances were sufficient and the main focus was not in the printed interconnects. In further studies, the reason for the difference between the measured and reported sheet resistance values should be explored. The thicknesses of the interconnects for example might have an influence on the measured sheet resistance but they were not measured within the framework of this thesis. On the other hand, the thickness of the screen correlates directly to the thickness of the interconnects and the screen was ordered based on the recommendations provided in the datasheet of the ink.

4.3 Initial Electrical Performance of the Adhesive Joints

Before implementing the strain tests, the initial electrical performance of the adhesive joints was evaluated. Because many types of adhesives were used, there were also various manufacturing processes. Every process needed to be optimized and the best parameters needed to be found in order to provide both the electrical connections and the mechanical support for the connections.

There were two critical phases during the attachment process: the batching of the adhesive and the placement of the component. Common to all adhesive bonding methods the component placement had to be done carefully. The component needed to be straight enough in order to confirm that all the contacts land on the pads. However, the bare carefully placement was not enough but the component was not allowed to move either when the pressure was applied on the component during the bonding process. An overly much amount of the NCA caused risk that there is adhesive also between the pads and all the connections cannot be formed. On the other hand, if there was too little NCA, the adhesion might have been insufficient and the contacts would not have enough support to withstand all the stresses and the strains. The same problems existed also with the underfill. Moreover overly much ICA could have caused short-circuits between the contacts. With ACF, the batching was not a problem because of its form. The ACF only needed to be cut to the right size and placed on the substrate.

The aim was to manufacture five sufficient samples of each combination of the adhesive and the substrate. Due to the component, four independent measurements per a sample were able to be implemented. The sufficient sample meant that all the joints of the sample were formed and the measured resistance of the channels had lower value than 110 Ω. In particular the resistances of the ACF joints could change within days if the joints were not properly formed. For ensuring that the joints are properly formed, the samples were manufactured on a different day than the tests were implemented. The variation

between the measured resistances of the adhesive joints is shown in Figure 26. The resistances were measured immediately before the tests.

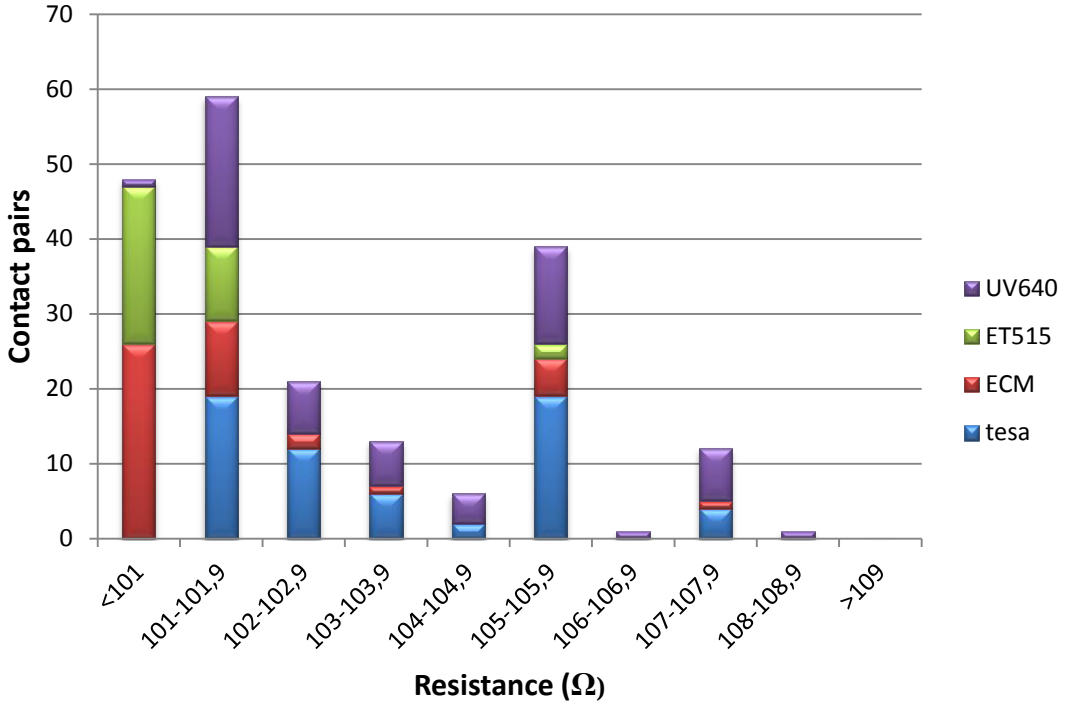

Figure 26. *The initial resistances of the samples*

In the measurements of Figure 26, the 4-point measuring was used in order to minimize the resistances of the printed wires. However, approximately a 15 mm part of the wires on both sides of the component is included in the measurement results. Those parts could be noticed in Figure 23. Typically, the sufficient joints with NCAs had lower resistance values than the sufficient joints with ICA or ACF.

4.4 Electromechanical Performance of the Adhesive Joints

The electromechanical performance of the joints was evaluated by two different kind of test. The first test was the cyclic stretching test and it was implemented for all the successful combinations of the adhesive and the substrate. For the one-time elasticity test, only the best combination based on the cyclic stretch test was chosen. Both tests were implemented with Tinius Olsen H5KT Benchtop Tester –based setup.

4.4.1 Cyclic Stretching

During the cyclic stretching test, the samples were stretched 10 % for 500 times. The resistances of the samples were measured continuously during the stretching. There were a lot of differences between the adhesives but the performance of the samples with the same adhesive and the same substrate also provided variable results. In Figure 27 is

presented an example of the resistance variation of one resistor during the test. The lower edge of the curve represents the resistance values when the strain is 0 %. In proportion, the upper edge of the curve shows the resistance at 10 % strain. In addition, the measurement was continued for ten minutes after the last cycle.

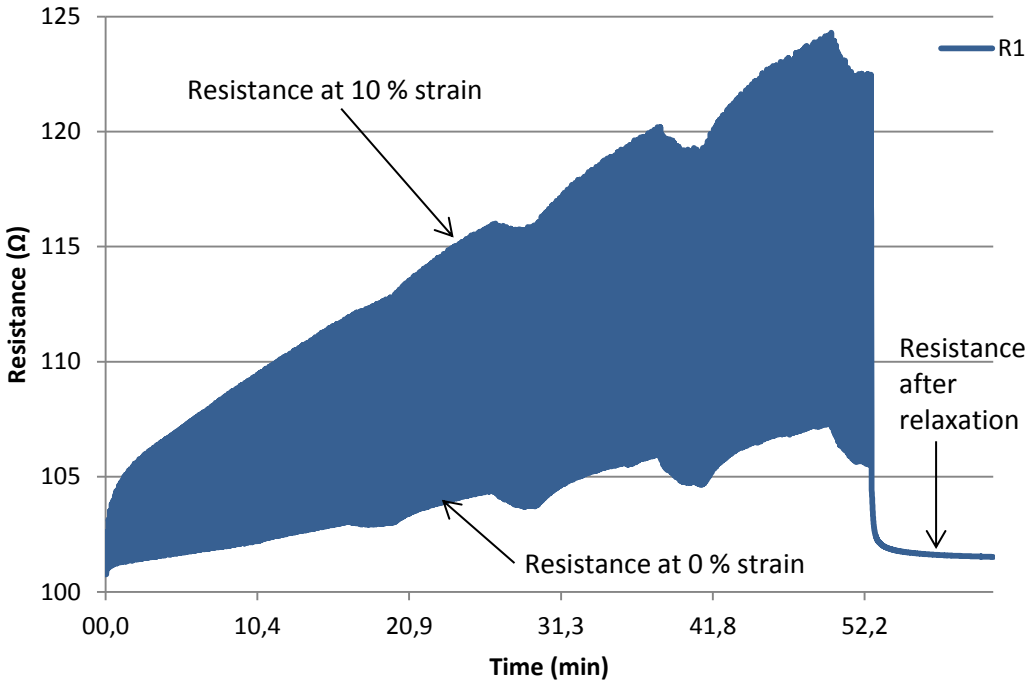

Figure 27. *The behavior of the resistance during cyclic strain test*

As can be seen in Figure 27, the resistance of the connection increases during every stretch cycle and when the stretch is removed the resistance decreases close to its initial value. When the test is progressed, the resistance increases more during the stretch cycles. However, TPU is a time-invariant material, so when the stretch rate is high, TPU does not have time to return to its initial shape. Then either the interconnects cannot return so the resistance does not reach its initial value between the cycles. However, when the joints of the sample were sufficiently mounted, the increase was moderate. For an example, when the initial resistance of a measured channel was close to 101 Ω, the joint typically survived the cyclic stretch with a sufficient increase in the resistance. By contrast, the joints with higher initial resistances tended to lose the connection or at least they had higher increases in the resistance. Although there were connection losses there was no visible breakage or changes in the adhesive joints.

In the resistance curve of Figure 27, there was deviation in the values at the time of 20, 30, 40 and 50 minute. The deviations referred to the behavior of H5KT because those points were also noticeable in the other resistance curves. However, the decreases of the resistance during the deviation points were at the highest roughly 1 Ω. That has probably affected the highest resistance value of the resistance curves but most probably they did not affect the breakage of the connections.

In Figure 28, the best and the worst resistance values of the same sufficient sample during one cycle are presented. The best cycles, when the resistances had the lowest increases, were measured during the first cycle of the test. The highest resistance values were reached during the last part of the test.

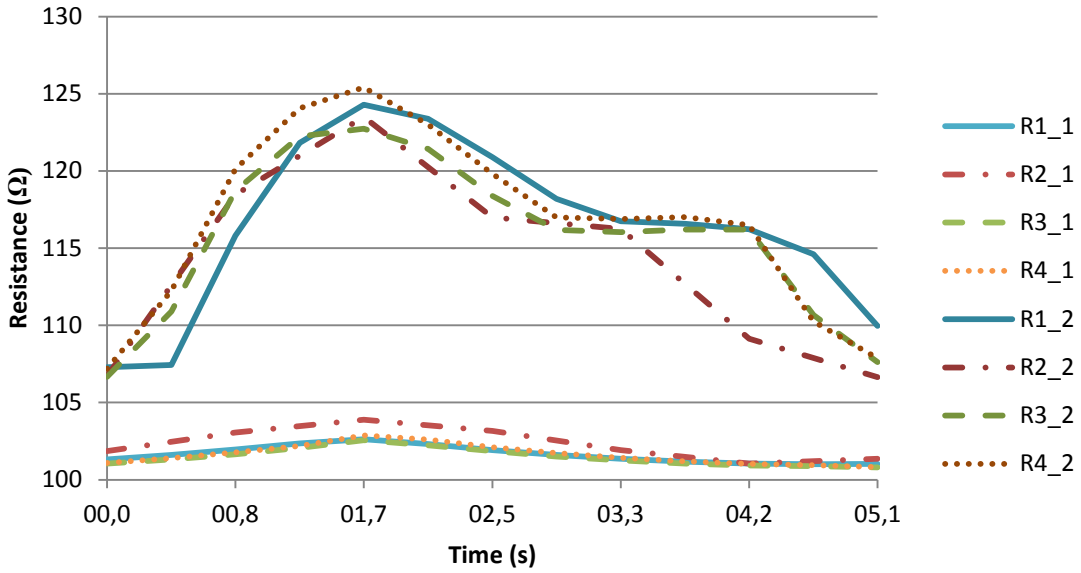

Figure 28. *The best cycle (R1_1-R4_1) and the worst cycle (R1_2-R4_2) of an unbroken sample*

In Figure 28, the best resistance curves are marked as R1_1–R4_1 and respectively the worst resistance curves are marked as R1_2–R4_2. In case of the curves of Figure 28, the biggest values of the best curves varied between 102.6 Ω and 103.9 Ω. Correspondingly the highest values of the worst cycles varied between 122.7 Ω and 125.4 Ω.

In good samples, the increase in the resistance value was between 9.14 % and 33.59 % depending on the adhesive and the substrate. At least a part of the resistance increase results from the resistance increase of the printed interconnects. The magnitude of that could be evaluated by printing a test pattern without the place for the component and implementing the same strain test for the printed interconnects. On the other hand, the rigid component and the adhesive may cause breakage in the interface between the adhesive and the interconnect.

In Figure 29 is collected more data about the worst cycles of all contact pairs. The results are itemized by the adhesives and the substrate materials. The bar chart of minimum resistances reflects the maximum resistances of the good samples. Overall, the increase of the resistances was lower in sufficient samples when rather TPU1 than TPU2 was used as the substrate material as can be seen from the minimum resistance chart in Figure 29. On the other hand, the connections on TPU1 had more tendencies to break than the connection on TPU2 which can be seen from the other charts in Figure 29.

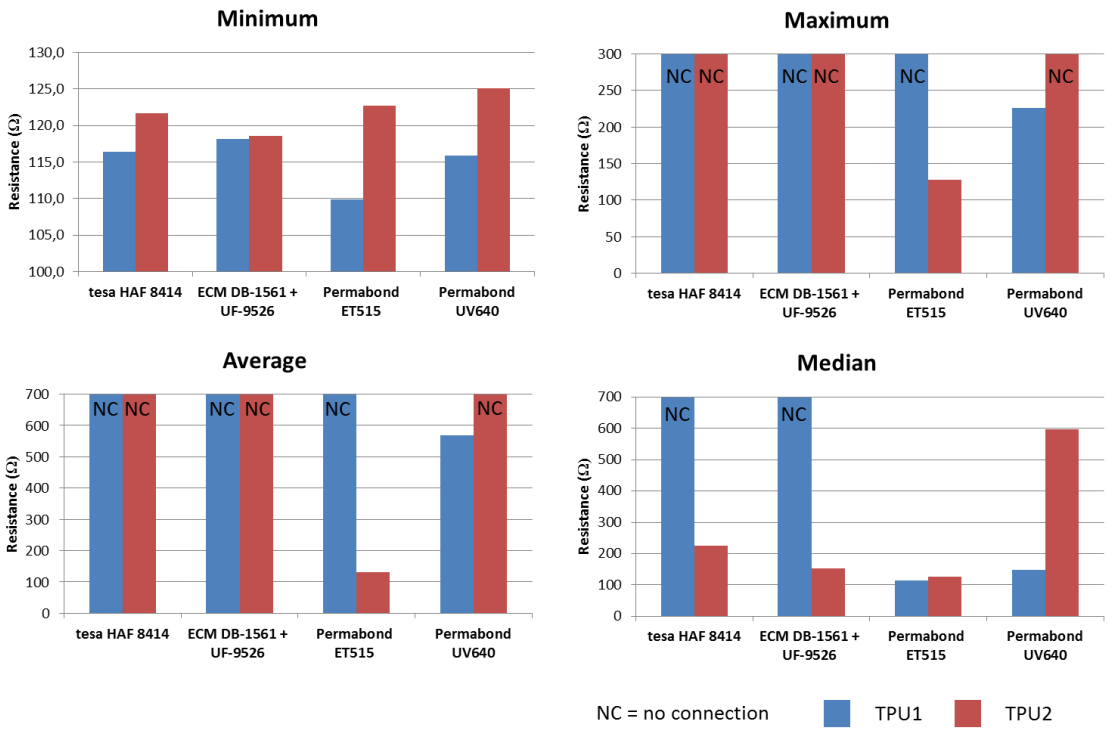

Figure 29. *The minimum, the maximum, the average and the median resistance of the worst cycles*

The results of the cyclic strain test are listed in Table 6. The results are given in two forms. Because one sample consists of four pairs of contacts all the pairs are processed individually. However, the sample will not be able to be acceptable if all the contacts are not durable. So, the other part of Table 6 considers the whole sample. When a pair of contacts is good, the resistance of the connections increases moderate. A sufficient pair of contacts means that the resistance stays under 500 Ω and the connection maybe lost only temporally less than ten times. In case of a bad pair of contacts, the connection is lost several times or even permanently.

Table 6. *The quality of the contacts and the samples.*

		Pair of Contacts			**Sample**		
		Good	**Sufficient**	**Bad**	**Good**	**Sufficient**	**Bad**
tesa	**TPU1**	2	5	13	0	0	5
	TPU2	8	7	5	0	2	3
ECM	**TPU1**	2	3	15	0	0	5
	TPU2	10	3	7	0	0	5
ET515	**TPU1**	18	0	2	3	0	2
	TPU2	20	0	0	5	0	0
UV640	**TPU1**	10	10	0	1	4	0
	TPU2	4	13	3	0	3	2

Based on the data in Table 6, the combination of ET515 and TPU2 was the only one that provided only good samples. The performance of ET515 was good also on the other substrate, TPU1. Although good pairs of contacts by other adhesives were also created, only the NCAs were able to create completely good samples. By contrast, all the samples with the ICA and underfill by ECM failed although there were some good pairs of contacts. One notable thing about the results is that the most of the failures did not mean a permanent loss of the connection but temporary.

In general, the resistances had decreased close to their initial resistance values already 10 minutes after the strain test. The resistances of the samples were measured again after at least one day had past and the most of the resistances were decreased even more. The changes between the lastly measured resistances and the initial resistances are modelled in Figure 30.

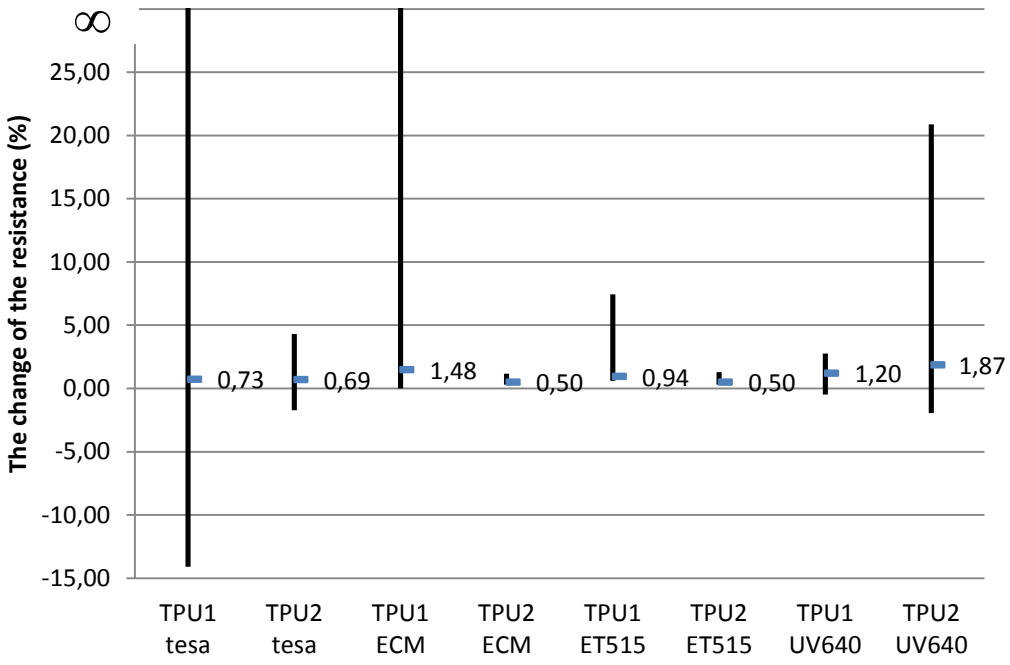

Figure 30. *The minimum, the maximum and the median of the returned resistance compared with the initial resistance values*

In Figure 30, the positive values mean that the resistance is higher than the initial resistance was. In proportion, the negative values stand for decrease in the resistance value. The negative values can be explained by a bad initial joint that has been reshaped better during the strain test. In addition, the median values of the resistance changes are marked in Figure 30. They vary between 0.5 % and 1.87 %. The ICA together with the undefill and ET515 on TPU2 performed the best. The performances of the ICA together with the underfill and the ACF on TPU1 were the weakest by providing some contact pairs without the connection after the strain test.

After the cycle test, one more cycle was implemented. Based on that last cycle, the program provided the proportionality of the extension to the force. An example of that is shown in Figure 31. During the cycle test, the sample stretches slightly permanently. So, when the graph is drawn after the cycles, the force starts to increase only after the sample is straightened.

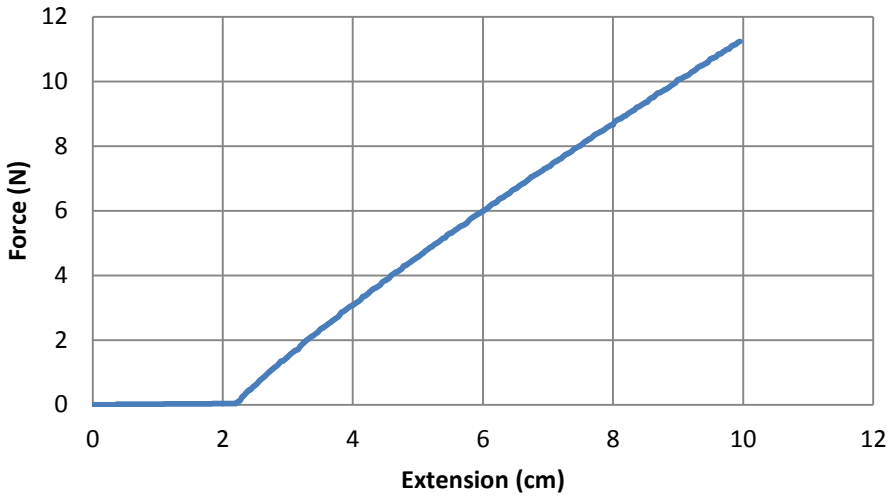

Figure 31. *An example of the proportionality between the force and the extension after cyclic stretching test*

The maximum stretching forces of the last cycles varied between 9 N and 13.5 N. Typically TPU1 required less force than TPU2 as can be seen from Figure 32. That was also expected because TPU2 is thicker than TPU1. In addition, TPU1 is more elastic than TPU2.

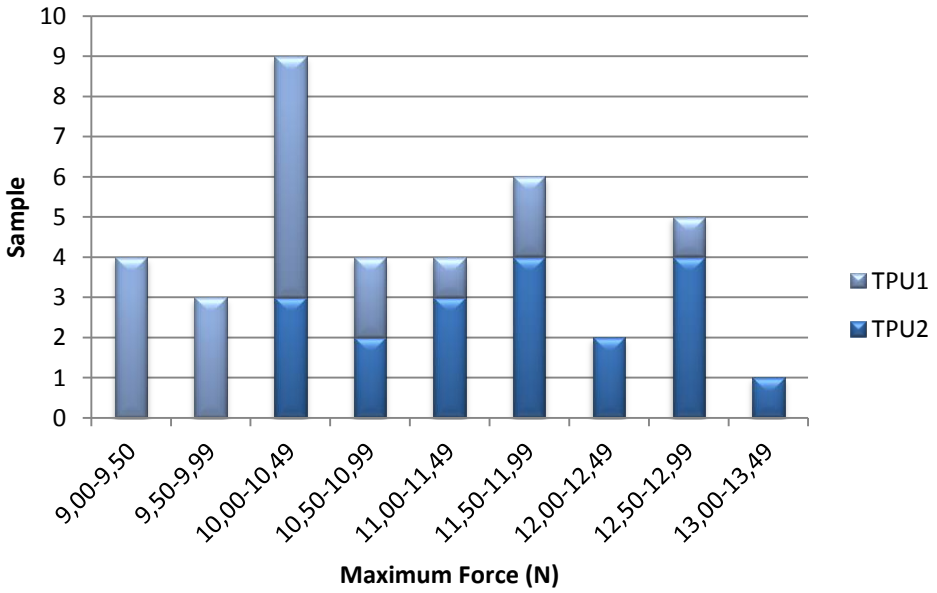

Figure 32. *The variation of the stretching forces*

In conclusion, only the joints made by ET515 on TPU2 qualified the cyclic stretching test. Also, the other NCA performed sufficiently but the performance of the ICA together with the underfill and of the ACF were insufficient. In the future the joints of ACFs and ICAs should be further studied. In addition, all the bonding processes needs to be more optimized in order to provide more equable quality for the adhesive joints. On the other hand, the reason for the resistance increase could be further explored by implementing the strain test for the samples with only the printed interconnects without the place for the component.

4.4.2 One-Time Elasticity

The one-time elasticity test was implemented only to the combination of the substrate TPU2 and the adhesive ET515 because they performed the best in the cyclic stretching test. In the test, the sample was stretched with a constant speed, 20 mm/min. The resistances of four channels were measured continuously during the stretching. In addition, the measuring was monitored in real time so when the connections were lost the extension points could be marked down. After all the connections were lost, the measuring was continued in order to ensure that the connections are lost permanently. In Figure 33, is shown an example of the proportion of the extension to the resistance during the stretching.

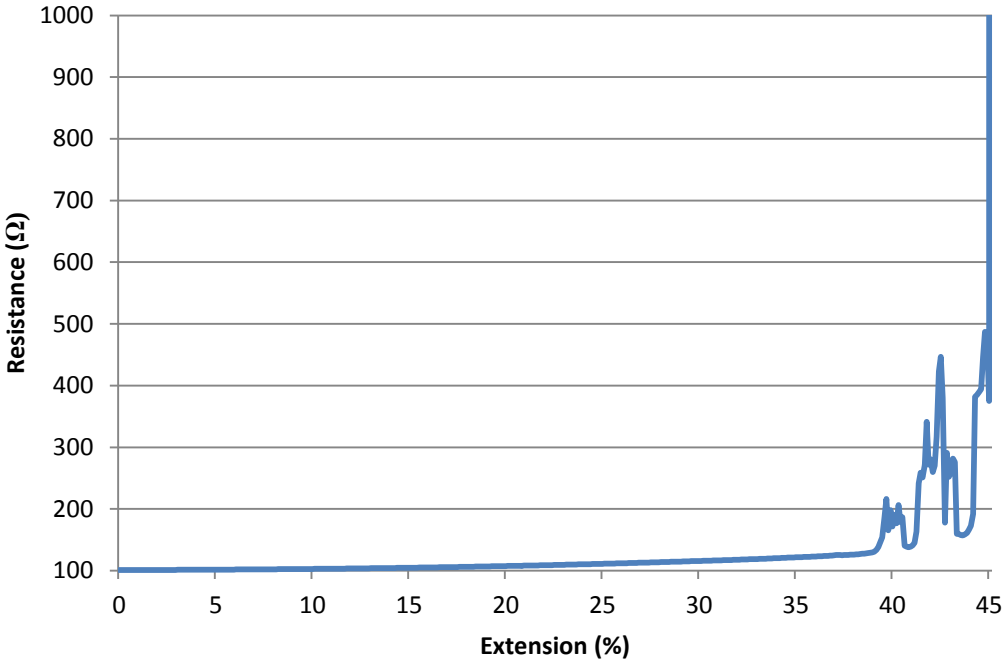

Figure 33. *The proportion of the extension to the resistance during stretching*

In Figure 33, the resistance increases moderate to the extension of 39 %. After that there are a couple of rapid increases before of the rapid loss of the connection. That phenom-

enon occurred also with the most of the other contacts. The break point has been defined to the point when conductivity got lost permanent.

The variation between the maximum extensions of the contact pairs is presented in Figure 34. All five samples withstood at least the strain of 20 %. In addition, three samples withstood strain of over 30 %. The breaking order of the contacts was irregular. Three of the samples broke first in the middle of the component and other two in the edges of the component.

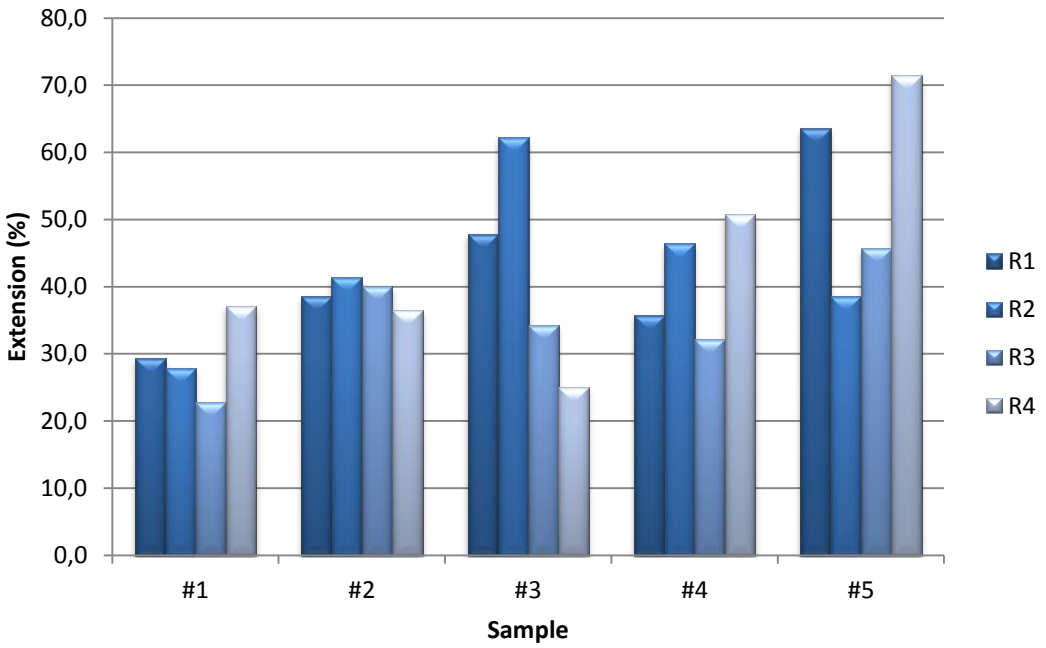

Figure 34. *The maximum extension of the contact pairs*

Also, the strain forces were measured during the stretching. In Figure 35 is presented the proportion of strain forces to the extension. Because the measurements were finished soon after all the connections were lost, also the force curves have different heights. However, the curves equal to each other fairly good. Only the force that is used to stretch the sample 5 seems to be a little higher. However, exactly the sample 5 withstood the highest extension.

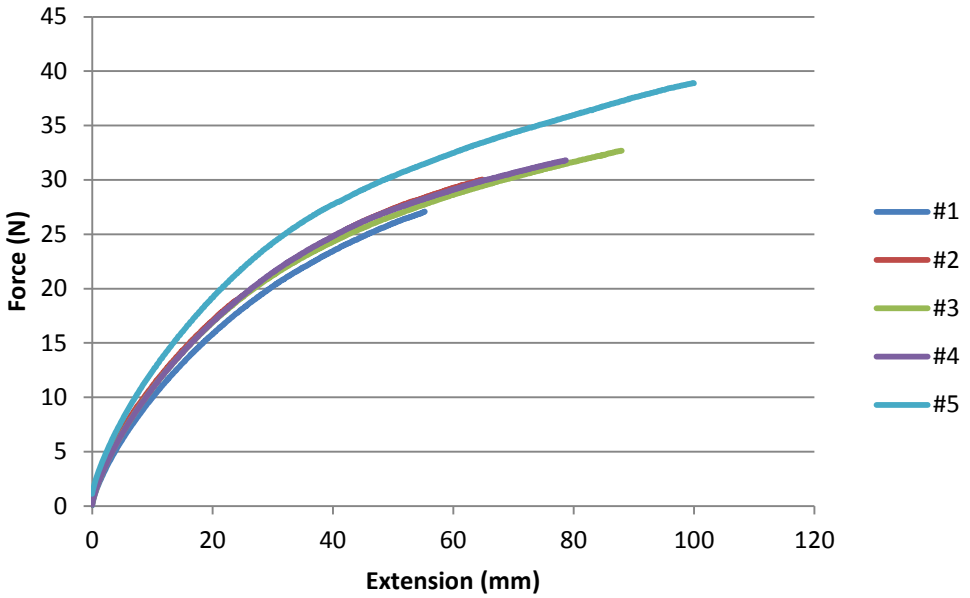

Figure 35. *The relation between the strain forces and the extension*

In conclusion, five samples provided the variable result from the one-time elasticity test. Although all samples withstood the extension of 20 %, the variation of the extensions that the pair of contacts withstood varied between 22.9 % and 71.4 %. In Future, bigger lots should be tested in order to explore if the performance of the samples is as random as this test showed. Also, the influence of the stretch rate to the performance should be investigated.

4.5 Performance of the Custom-Made Test Setup

The custom-made test setup was designed and manufactured for this thesis from the beginning so the performance of the setup is investigated in this chapter. H5KT –based test setup was used as an aid in the evaluation although the custom-made test setup provides differently shaped stretching. Five test samples for both test setups were manufactured and they were stretched until all the connections were lost. In Figure 36 is presented an example of the proportion of the resistance to the time during the stretching test with the custom-made test setup.

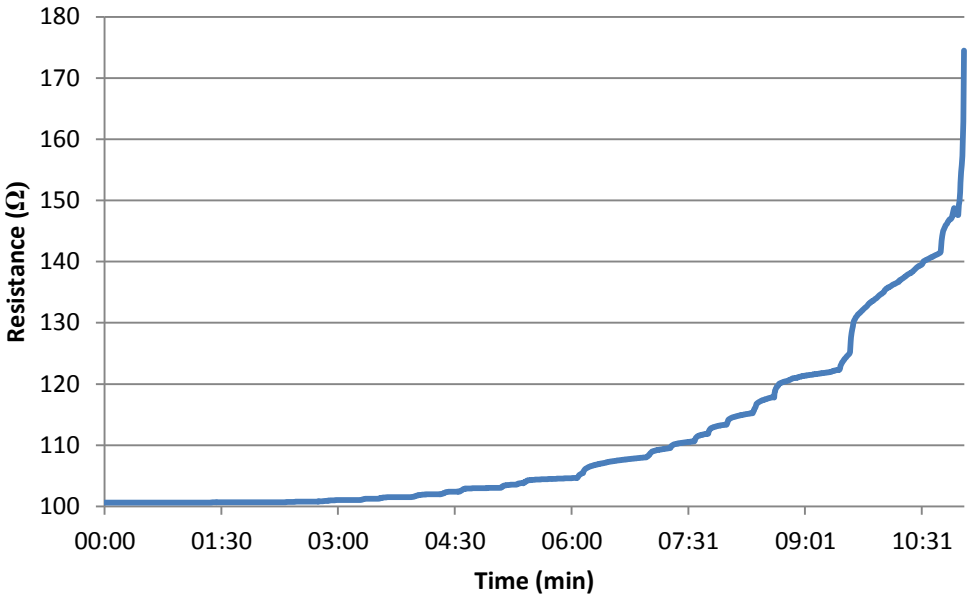

Figure 36. *The proportion of the resistance to the time under the strain caused by the custom-made test setup*

The increase in the resistance in Figure 36 is quite exponential and it is similar to the corresponding curve of H5KT that is shown in Figure 37. However, the points when the compressed air was increased and the stretcher was moved can be seen in Figure 36 as little steps whereas the increase in the resistance with H5KT is smoother. In addition, because the custom-made test setup is fully manual the stretching rate was either not constant.

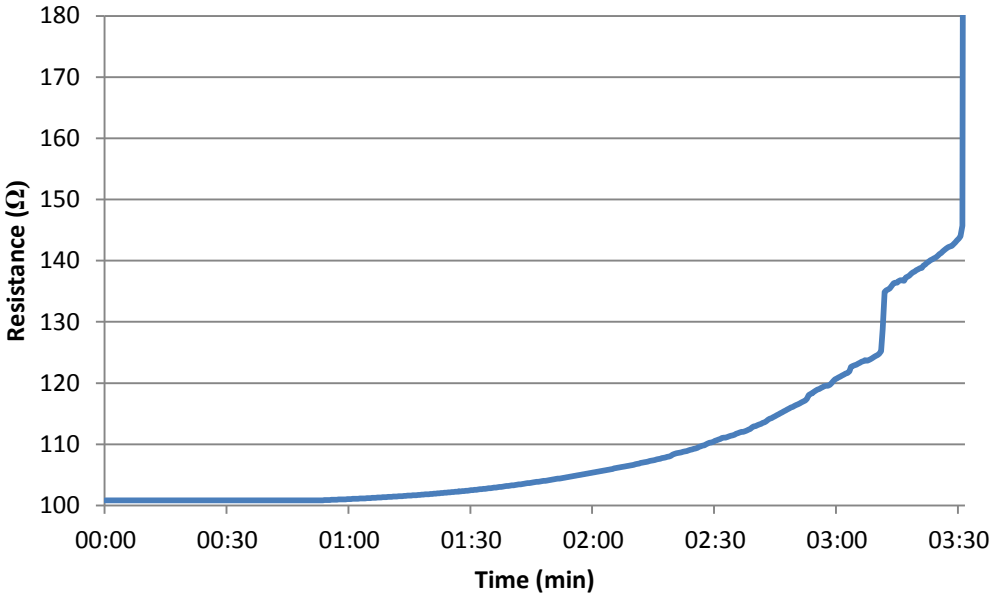

Figure 37. *The proportion of the resistance to the time under the strain caused by Tinius Olsen H5KT –based setup*

The breakdown of the sample is determined to be the phase when the first pair of contacts loses the connection. The breakdown comparison of the setups is presented in the right part of Figure 38. As for the left part, it represents the average extension of the samples. On average, the samples withstood the larger extensions with H5KT –based setup than with the custom-made setup which was also expected.

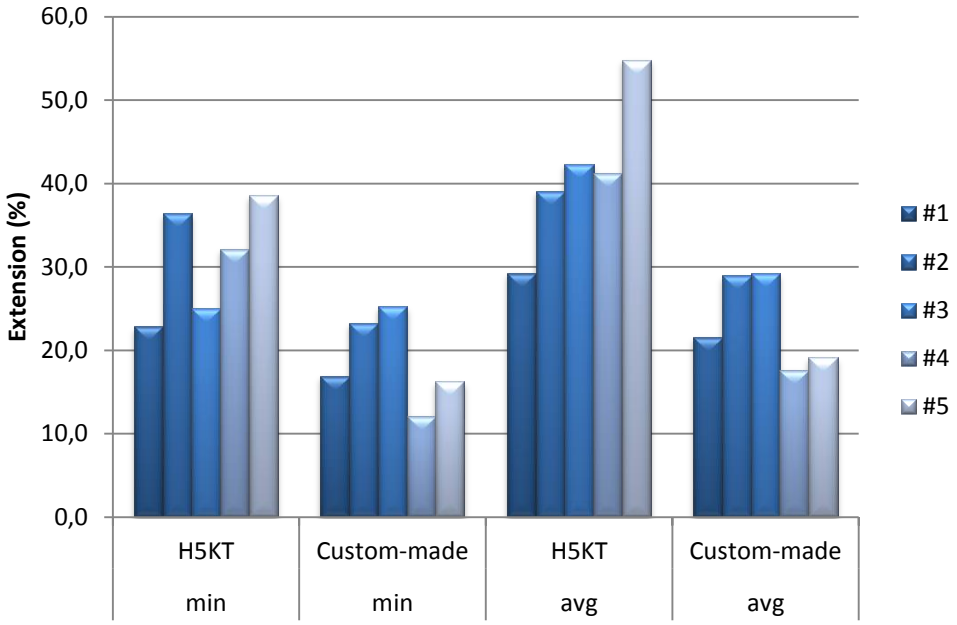

Figure 38. *The breakdown extension of the samples and the average extension of the sample*

In both strain tests implemented by H5KT, the component and the adhesive did not start to disengage from the substrate during the stretching. However, this phenomenon was typical in the one-time elasticity test with the custom-made test setup. The substrate tended to stretch whereas the component and the adhesive did not stretch at all. So, when the stretching occurred in every direction, the adhesive joint experienced more stress than when the stretching was only uniaxial. That turned up so that the adhesive joint gave way and some of the outermost pads stretched away underneath the component. That phenomenon is shown in Figure 39.

Figure 39. *The breakdown of the adhesive joints under strain in custom-made test setup*

In conclusion, the performance of the custom-made test setup was as expected. The set-up enabled the same amount of strain in every direction so the samples also lost the connections with a less uniaxial measured extension than was measured with the other setup.

However, in further tests the setup should be developed. With manual control, the tests made with the custom-made test setup never equal exactly each other so the reproducibility of the test is weak. In addition the setup is not suitable for cyclic tests such as this. The setup also requires some automatic measuring for the extension. The curvature of the substrate underneath the component was not possible to remove totally but if wanted it could be reduced for example by replacing the stretcher with a new stretcher with a shorter diameter. Although the friction between the stretcher and the substrate did not influence the stretching in this test, also it needs to be reconsidered when choosing the material for the new stretcher. Moreover the friction might cause problems when a cyclic test with a bigger stretch rate is implemented.

5. CONCLUSIONS AND PROPOSALS FOR FUTURE WORK

In this thesis, the main aim was to manufacture and evaluate adhesive joints of a different kind between a stretchable substrate and a rigid component. Another aim was to design and implement a custom-made setup that enables stretching the same amount in every direction at the same time. The aims were reached.

In Chapter 2, the wearable and stretchable technologies were introduced. The stretchable electronics is a way to make the wearable electronics unobtrusiveness to the user. For creating the stretchable electronics, the substrate needs to be stretchable. So, the mechanical properties of the stretchable materials were discussed and various material possibilities for the stretchable substrate were presented. Also the ways and materials to create stretchable wirings were presented. In addition, the principles of three types of adhesives (ICA, ACA and NCA) and their bonding processes were studied. The adhesive joints were compared with the conventional solder joints and the disadvantages and the advantages of the adhesive joints were discussed.

Chapter 3 concentrates on the methods and devices that are used in this thesis. First, the screen-printing process and the materials for it were presented. Four different adhesives were used in this thesis for creating the adhesive joints. All of them had different kind of the curing process. For the UV-curable adhesive, an UV-curable device was designed and manufactured. Two different devices for the ACF bonding process were studied. In addition, the equation for measuring the sheet resistance of the printed interconnects was led. Lastly in Chapter 3, the test setups were presented. Tinius Olsen H5KT Benchtop Tester –based setup was used in both the cyclic strain test and the one-time elasticity test. The setup includes four 4-point resistance measuring units which were used in the continuous resistance measurements during the strain test. The stretching was automatic when the parameters were given to the strain test controlling computer. The software also logged the data of the stretching force. In addition, the custom-made test setup was designed and manufactured. Based on the first version of the test equipment, some further development was implemented like the adding of the compressed air.

The corresponding results to the tests were presented and discussed in Chapter 4. The quality of the screen-printing process was roughly evaluated and two main quality issues were found. Firstly, there were a lot of impurities because the process was not implemented in a clean room. The second issue occurred with one TPU, Platilon. The printed wirings on Platilon did not withstand even slight strain without cracking. Next,

the initial performance of the printed interconnects was evaluated by measuring their sheet resistances. The average of the measured sheet resistances was 32.1 Ω/□ which was higher than in the datasheet of the ink was reported. However, the sheet resistances were sufficient for this thesis so the difference was not further studied. The initial electrical performance of the created adhesive joints was also evaluated. The resistance measurements included the resistance of the component, of the joints and of the small parts of the printed wirings. Only the samples that had the initial resistance of the channels lower than 110 Ω were accepted to the strain tests. The sufficient samples were managed to manufacture with four of the six initial adhesives. So, the adhesives that were used in the first strain test were ICA DB1561 by together with the underfill UF-9526, tesa HAF 8414 ACF and the NCAs by Permabond, ET515 and UV640. In addition, the substrate materials in the first test were TPU1 and TPU2.

Two strain tests were implemented and their results were presented and discussed in Chapter 4. The first was the cyclic strain test that was implemented by Tinius Olsen H5KT Benchtop Tester –based setup. During the test, four channel of the sample were measured continuously by the 4-point resistance measurement. The samples were stretched uniaxial 10 % for 500 times during the cyclic strain test. The increase in the resistance in the sufficient joint was from 9.14 % to 33.59 % depending on the adhesive and the substrate. The lowest increases appeared with the combination of ET515 and TPU1 and respectively the highest increases with the combination of the ACF by tesa and TPU2. However, the variation between the samples was high, even with the samples with the same adhesive and substrate combination. The combination of ET515 and TPU2 was the only one that provided only good samples. Altogether, the performance of the ICA together with the undefill and of the ACF was insufficient. Every sample made by the ICA and underfill included at least one contact pair that lost the connection during the stretching. However, most of the connection loses were only temporary.

For the best combination, TPU2 with ET515, the one-time elasticity test was implemented with H5KT –based setup. Also in this test the resistances of four channels were measured continuously during the stretching. The resistances increased evenly first but when the breaking point was approached it started to increase rapidly. All five samples that were tested withstood at least the extension of 20 % and three of them withstood over 30 % extension. However, the stretching was continued until the channel of the sample lost the connection. One of the contact pairs last even extension of 71.4 %.

Finally, Chapter 4 also included the comparison between H5KT –based setup and the custom-made test setup in order to evaluate the performance of the custom-made test setup. In the comparison, the one-time elasticity test was implemented also with the custom-made setup for five samples. The stretching situation was rougher because the substrate was stretched in every direction at the same time. That was noticed on the sides of the component. The connections broke because the substrate stretched under-

neath the component and the adhesive gave away. Thus, in general the samples lost the connections sooner with the custom-made test setup which was also expected.

For future work, it is proposed that the cracking of the ink on Platilon is further studied. It could be started by exploring the successful print samples manufactured with the different screen-printer. Another way is to design new screen for the screen-printer. The test screen could include traces with different widths. In addition, the reason for the high sheet resistance of the printed interconnects needs to be figured out. It might be a result from the thickness of the printed traces.

In Future, also the bonding processes of the adhesives needs to be further researched. Especially, the ACF bonding process requires additional exploring because there are also other issues than the parameters that need to be taken account. The component with pure thin solder contacts may be the reason for insufficient joints. In addition the interest of the wearable technologies is not just attaching one component to stretchable substrate but a component island. Thus, next a test island could be designed and implemented. Then, the functionality of the ACFs could be reconsidered.

In addition, more strain tests should be implemented with different parameters. The one-time stretch test should be implemented for different substrates and adhesives. On the other hand, it is proposed that the reason for the resistance increase is further studied. For that, a new test pattern without a place for the component should be done so that the resistances of the pure printed wires could be measured under the cyclic stretching. Also, the relevance of the stretch rate in both the cyclic and the one-time elasticity test should be evaluated. Lastly, the custom-made test setup needs further development in order to for example improve its usability and reproducibility. With the automatic control of the compressed air and stretcher, the setup could be used also in cyclic stretching tests. Another issue to be considered is to make the measuring of the extension automatic.

REFERENCES

[1] H. Peter, H. James, D. Raghu, and H. Glyn, Wearable Technology 2015-2025: Technologies, Markets, Forecasts, *IDTechEx*, 2015.

[2] T. Sterken, J. Vanfleteren, T. Torfs, M. O. de Beeck, F. Bossuyt, and C. Van Hoof, Ultra-Thin Chip Package (UTCP) and stretchable circuit technologies for wearable ECG system., *33rd Annu. Int. Conf. IEEE Eng. Med. Biol. Soc.*, pp. 6886–6889, 2011.

[3] S. P. Lacour, Stretchable Thin-Film Electronics, *Stretchable Electron. (ed. T. Someya)*, pp. 81–109, 2013.

[4] M. Gonzalez, Y.-Y. Hsu, and J. Vanfleteren, Modeling of Printed Circuit Board Inspired Stretchable Electronics System, *Stretchable Electron. (ed. T. Someya)*, pp. 143–159, 2013.

[5] J. Suikkola, T. Björninen, M. Mosallaei, T. Kankkunen, P. Iso-ketola, L. Ukkonen, J. Vanhala, and M. Mäntysalo, Screen-Printing Fabrication and Characterization of Stretchable Electronics, *Nat. Publ. Gr.*, no. April, pp. 1–8, 2016.

[6] T. Liimatta, E. Halonen, H. Sillanpää, J. Niittynen, and M. Mäntysalo, Inkjet Printing in Manufacturing of Stretchable Interconnects, pp. 1–85, 2014.

[7] K. Tehrani and M. Andrew, Introduction to Wearable Technology What is Wearable Technology? What are Wearable Devices?, *Wearable Devices*, 2014. [Online]. Available: http://www.wearabledevices.com/what-is-a-wearable-device/. [Accessed: 17.02.2016].

[8] J. Kim, B. Keane, J. S. Park, and W. S. Kim, Stretchable Inter-Connection by Printed Silver Nano-Ink *, *IEEE Int. Conf. Nanotechnol.*, pp. 412–415, 2014.

[9] Lesson: Mechanics of Elastic Solids, *Teach Engineering curriculum for k-12 teachers*, 2011. [Online]. Available: https://www.teachengineering.org/view_lesson.php?url=collection/cub_/lessons/cub_surg/cub_surg_lesson02.xml. [Accessed: 19.01.2016].

[10] True Stress - True Strain Curve: Part One, *Total Materia*, 2010. [Online]. Available: http://www.totalmateria.com/page.aspx?ID=CheckArticle&site=kts&NM=280. [Accessed: 20.01.2016].

[11] K. D. Harris, A. L. Elias, and H. J. Chung, Flexible electronics under strain: a review of mechanical characterization and durability enhancement strategies, *J. Mater. Sci.*, vol. 51, no. 6, pp. 2771–2805, 2016.

[12] M. Adler, R. Bieringer, T. Schauber, and J. Günther, Materials for Stretchable Electronics Compliant with Printed Circuit Board Fabrication, *Stretchable Electron. (ed. T. Someya)*, pp. 161–185, 2013.

[13] Product Information Platilon® U Highly Elastic Polyurethane Films, *Covestro Deutchland AG*, 2015. [Online]. Available: http://www.films.covestro.com/products/platilon.aspx/. [Accessed: 26.02.2016].

[14] Technical Data PLATILON ® U Highly Elastic Polyurethane Films, 2012. .

[15] Technical Data of TPU2.

[16] Technical Data of TPU1, 2011.

[17] D.-H. Kim, J. Xiao, J. Song, Y. Huang, and J. A. Rogers, Stretchable, Curvilinear Electronics Based on Inorganic Materials, *Adv. Mater.*, vol. 22, no. 19, pp. 2108–2124, 2010.

[18] J. Song and S. Wang, Theory for Stretchable Interconnects, *Stretchable Electron. (ed. T. Someya)*, pp. 3–29, 2013.

[19] B. E. Kahn, Patterning Processes for Flexible Electronics, *Proc. IEEE*, vol. 103, no. 4, pp. 497–517, 2015.

[20] S. Khan, L. Lorenzelli, R. Dahiya, and S. Member, Technologies for Printing Sensors and Electronics over Large Flexible Substrates : A Review, *IEEE Sens. J.*, vol. 15, no. 6, pp. 3164–3185, 2015.

[21] A. Hobby, Printing Thick Film Hybrids, *DEK Printing Machines Ltd.*, 1997. [Online]. Available: http://www.gwent.org/gem_thick_film.html. [Accessed: 28.12.2015].

[22] T. D. Sheet, CI-1036, Highly Conductive & Highly Flexible Silver Ink, Technical Data Sheet, *ECM Tech. Data Sheet*, no. 740, 2010.

[23] B. Salam and B. K. Lok, Solderability and reliability of printed electronics, *15th Int. Symp. Phys. Fail. Anal. Integr. Circuits*, pp. 1–4, 2008.

[24] Comparison of lead-free solders, *Interflux Electronics*. [Online]. Available: http://www.interflux.com/sites/default/files/documents/en/General info - lead free alloys.pdf. [Accessed: 17.05.2016].

[25] L. Frisk, Study of Structure and Failure Mechanisms in ACA Interconnections Using SEM, *Scan. Electron Microsc.*, pp. 491–516, 2012.

[26] L. Frisk, S. Lahokallio, M. Mostofizadeh, J. Kiilunen, and K. Saarinen, Reliability study of isotropic electrically conductive adhesives under thermal cycling testing, *2013 IEEE 63rd Electron. Components Technol. Conf.*, pp. 1794–1799, 2013.

[27] DB-1561, Technical Datasheet, *ECM Eng. Conduct. Mater. LLC*, 2010.

[28] UF-9526, Technical Datasheet, *ECM Eng. Conduct. Mater. LLC*, 2010.

[29] K. Motoki, M. Oyama, T. Imai, T. Ishii, M. Kimata, H. Horita, N. Sasaki, I. Kobayashi, T. Yokoyama, A. Ono, S. Kodate, S. Suzuki, Y. Ono, and M.

Kurosawa, Connecting Technology of Anisotropic Conductive Materials, *Fujikura Tech. Revie*, 2002.

[30] POLYKO, Polymeerimateriaalit elektroniikassa, 2010. [Online]. Available: https://www.tut.fi/ms/muo/polyko/materiaalit/TTY/Elektroniikka/EPDF/Polymeerimaterialien_sovellukset_eletroniikassa.pdf. [Accessed: 12.01.2016].

[31] M. A. Uddin, M. . Y. Ali, and H. . P. Chan, Achieving Optimum Adhesion of Conductive Adhesive Bonded Flip-Chip on Flex Packages, *Adv. Mater. Sci.*, vol. 21, pp. 165–172, 2009.

[32] HAF 8414, Datasheet, *tesa* ®, 2015. [Online]. Available: http://www.tesa.com/industry/electronics/smart_card/chip_fixation/download/5171771/11905297/master-pi.pdf. [Accessed: 04.02.2016].

[33] 7303 Anisotropic Conductive Film Adhesive, Datasheet, *3M*, 2007. [Online]. Available: https://multimedia.3m.com/mws/media/66294O/3mtm-anisotropic-conductive-film-7303.PDF. [Accessed: 04.02.2016].

[34] 9703 Electrically Conductive Adhesive Transfer Tape, Datasheet, *3M*, 2015. [Online]. Available: http://multimedia.3m.com/mws/media/66235O/3m-electrically-conductive-adhesive-transfer-tape-9703.pdf. [Accessed: 04.02.2016].

[35] T. Linz, M. Von Krshiwoblozki, and H. Walter, Novel packaging technology for body sensor networks based on adhesive bonding: A low cost, mass producible and high reliability solution, *2010 Int. Conf. Body Sens. Networks, BSN 2010*, pp. 308–314, 2010.

[36] K. Saarinen and L. Frisk, Changes in Adhesion of Non-Conductive Adhesive, *IEEE Trans. Components, Packag. Manuf. Technol.*, vol. 1, no. 7, pp. 1082–1088, 2011.

[37] ET515 Two-part Epoxy, Technical Datasheet, *Permabond ® Engineering adhesive*, 2014. [Online]. Available: http://www.permabondllc.com/TDS/ET515_TDS.pdf. [Accessed: 02.02.2016].

[38] UV640 UV-Curable Adhesive, Technical Datasheet, *Permabond ® Engineering adhesive®*, 2014. [Online]. Available: http://www.permabondllc.com/TDS/UV640_TDS.pdf. [Accessed: 02.02.2016].

[39] P. Foerster, T. Linz, M. Von Krshiwoblozki, H. Walter, C. Kallmayer, and R. Aschenbrenner, NCA flip-chip bonding with thermoplastic elastomer adhesives - Fundamental failure mechanisms and opportunities of polyurethane bonded NCA-interconnects, *2011 IEEE 13th Electron. Packag. Technol. Conf. EPTC 2011*, pp. 223–230, 2011.

[40] J. Suikkola, Printed Stretchable Interconnects for Wearable Health and Wellbeing Applications, p. 59, 2015.

[41] UV-LED, Series 400 - Ceramics, *OSA Opto Light*, 2010. [Online]. Available: http://www.farnell.com/datasheets/1305904.pdf. [Accessed: 03.02.2016].

[42] S. Enderling, S. Member, C. L. Brown, S. Smith, M. H. Dicks, J. T. M. Stevenson, M. Mitkova, M. N. Kozicki, A. J. Walton, and N. Si, Sheet Resistance Measurement of Non-Standard Cleanroom Materials Using Suspended Greek Cross Test Structures, *IEEE Trans. Semicond. Manuf.*, vol. 19, no. 1, pp. 2–9, 2006.